Work Order No. 582-18-81573-28
Contract No. 582-15-50417
Tracking No. 2018-09

Near-Real Time Exceptional Event Modeling
Final Report

PREPARED UNDER A CONTRACT FROM THE
TEXAS COMMISSION ON ENVIRONMENTAL QUALITY

The preparation of this report was financed through a contract from the State of Texas through the Texas Commission on Environmental Quality. The content, findings, opinions and conclusions are the work of the author(s) and do not necessarily represent findings, opinions or conclusions of the TCEQ.

Prepared for:
Mark Estes
Texas Commission on Environmental Quality
121 Park 35 Circle MC 164
Austin, TX 78753

Prepared by:
Jeremiah Johnson, Gary Wilson, Justin Bandoro,
Kurt Richman, Ling Huang, Ross Beardsley and Greg Yarwood

Ramboll
773 San Marin Drive, Suite 2115
Novato, California, 94998
www.ramboll.com
P-415-899-0700
F-415-899-0707

August 2018

RAMBOLL

CONTENTS

TABLES

FIGURES

LIST OF ACRONYMS AND ABBREVIATIONS

4HMDA8	4th highest 8-hour daily maximum ozone
BCs	Boundary Conditions
CAMS	Continuous Air Monitoring Station
CAMx	Comprehensive Air quality Model with extensions
CMAQ	Community Multiscale Air Quality Model
CO	Carbon Monoxide
CST	Central Standard Time
DFW	Dallas-Fort Worth Area
EBI	Euler Backward Iterative method
EDGAR	Emissions Database for Global Atmospheric Research
EPA	Environmental Protection Agency
EPS3	Emissions Processing System version 3
FIM	Fire Impact Modeling
FINN	Fire INventory from NCAR
GEOS	Goddard Earth Observing System
GDAS	GFS Data Assimilation System
GFS	Global Forecasting System
HGB	Houston-Galveston-Brazoria Area
HMS	Hazard Mapping System
HTAP	Hemispheric Transport of Air Pollution
ICs	Initial Conditions
IGBP	International Geosphere Biosphere Programme
ISD	Integrated Surface Data
LAI	Leaf Area Index
LI	Local Increment
LSM	Land Surface Model
mb	millibars
MDA1	daily maximum 1-hour average
MDA8	daily maximum 8-hour average
MEGAN	Model of Emissions of Gases and Aerosols from Nature
MODIS	Moderate Resolution Imaging Spectroradiometer
MOZART	Model for OZone and Related chemical Tracers
m	meter
MM5	Fifth-Generation Penn State/NCAR Mesoscale Model
MPI	Message Passing Interface
MSKF	Multi-Scale Kain Fritsch
NAM	North American Model
NASA	National Aeronautics and Space Administration
NCAR	National Center for Atmospheric Research
NCDC	National Climatic Data Center
NCEP	National Centers for Environment Prediction
NCL	NCAR Command Language

NDAS	NAM Data Assimilation System
NMB	Normalized Mean Bias
NME	Normalized Mean Error
NAAQS	National Ambient Air Quality Standard
NO	Nitric Oxide
NOAA	National Oceanic and Atmospheric Administration
NOx	Oxides of Nitrogen
NRT	Near Real-Time
OMP	Open Multi-Processing
PBL	Planetary Boundary Layer
PFT	Plant Functional Type
PM	Particulate Matter
$PM_{2.5}$	Particulate Matter < 2.5 ug m^{-3}
ppb	parts per billion
PPM	Piecewise Parabolic Method
Q-Q	Quantile-Quantile
RMSE	Root Mean Squared Error
RPO	Regional Planning Organization
RRTMG	Rapid Radiative Transfer Model for GCM applications
SIP	State Implementation Plan (for the ozone NAAQS)
TCEQ	Texas Commission on Environmental Quality
TOMS	Tropospheric Ozone Mapping Spectrometer
TUV	Tropospheric UltraViolet radiative transfer model
ug	micrograms
US	United States
WRF	Weather Research and Forecast model
WSM6	WRF Single-Moment 6-Class Microphysics Scheme
YSU	Yonsei University WRF planetary boundary layer parameterization

1.0 EXECUTIVE SUMMARY

Ramboll assisted the TCEQ by deploying a Near-Real Time Exceptional Event Modeling (NRTEEM) system that estimates ozone impacts for three potential sources of exceptional events in Texas: (1) biomass burning in Mexico and Central America; (2) stratospheric ozone intrusion; (3) anthropogenic emissions in Mexico. We tested the NRTEEM system during March – June 2018 and delivered model results via a website. The NRTEEM system delivers results with a 1-day lag to acquire biomass burning emissions that are derived from satellite observations of Earth.

The NRTEEM system uses the Weather, Research and Forecasting (WRF) meteorological model, the Comprehensive Air Quality Model with Extensions (CAMx) air quality model, biomass burning emissions from Fire INventory of NCAR (FINN) and anthropogenic emissions data provided by the TCEQ. Model configurations are similar to those used for the TCEQ's State Implementation Plan (SIP) modeling. This report describes the implementation of the 2018 NRTEEM system and our evaluation of system performance. We provide specific recommendations for future NRTEEM system improvements.

1.1 Updates from 2017 FIM System

In developing the NRTEEM system, Ramboll made the following updates from the 2017 FIM ozone modeling system:

1. Added two new potential sources of exceptional events: 1) stratospheric ozone intrusion and 2) Mexican anthropogenic emissions;
2. Added two new sensitivity simulations to evaluate model performance impacts from changes in dry deposition;
3. Re-speciated FINN fire emissions to simulate more realistic (rapid) NOx to NOy conversion in smoke plumes;
4. Expanded the NRTEEM website to display global air quality model concentrations and satellite imagery for detection of fire hotspots and smoke plumes;
5. Updated the website interface to animate any range of consecutive dates

1.2 Model Performance Summary

We performed quantitative and qualitative evaluation of WRF meteorological and CAMx ozone performance. Evaluation of WRF meteorological statistical metrics revealed that the NRTEEM system agreed as well or better with observations than the 2017 FIM system. The objective of the CAMx ozone model performance evaluation was to determine whether the alternative dry deposition schemes (Zhang and Zhang Mod) substantially impact or improve ozone performance. The Zhang run replaces the Wesely deposition scheme used in the base model with the Zhang deposition scheme. The Zhang Mod run modified the Zhang scheme in forested areas and over the ocean.

In general, the Zhang simulation results in higher ozone concentrations (due to lower ozone deposition) compared to the base model. Therefore, when the base model underestimates

ozone, the Zhang simulation tends to improve performance. The Zhang Mod simulation results in lower ozone concentrations compared to Zhang, which results in performance similar to the base model.

Next, we examined the local increment (LI) to MDA8 ozone as a way to measure the model's ability to estimate ozone production from emissions in a given metropolitan area. Overall, we found very little difference between the base and Zhang runs. Performance was found to be quite good in Dallas. Consistent with the previous FIM study (Johnson et al., 2017), we found persistent LI underestimates in Houston for both the base and Zhang runs. We evaluated background MDA8 ozone performance in Dallas and Houston and found that while the Zhang runs improved correlation, bias and error performance was mixed.

Finally, we examined relationships between modelled exceptional event impacts and base case model bias. If such relationships existed they might indicate that the modelled exceptional event impacts were themselves biased. We find no clear relationship between any of the exceptional event impacts and NRTEEM base case model bias.

1.3 Potential Exceptional Event Impact Summary

NRTEEM includes three sensitivity simulations to identify potential exceptional events. The first quantifies ozone impacts from biomass burning and found a potential exceptional event at the Camp Bullis monitor in San Antonio on April 28, 2018. During the high ozone period of July 25 – August 4, 2018, we found 67 occurrences where observed MDA8 ozone exceeded 70 ppb and NRTEEM fire impacts equalled or exceeded 0.7 ppb (1% of the NAAQS). These are potential fire contributions that might or might not be relevant to attainment for an area depending upon whether they are in the top four highest MDA8 observations at the end of the ozone season and whether the monitor ends up determining the attainment status for an area. The second simulation examines stratospheric ozone intrusions. While we find some measurable stratospheric ozone impacts in El Paso, the impacts did not occur when observed ozone was high so we did not find any potential exceptional events. The third simulation quantifies ozone impacts of Mexico anthropogenic emissions, which may not fit within the regulatory definition of an exceptional event, and we found two potential exceptional events at San Antonio and El Paso monitors.

The NRTEEM system implements and refines the photochemical grid model system used by the TCEQ for State Implementation Plan (SIP) modeling by modeling exceptional event impacts in a NRT mode. The system demonstrates usefulness by identifying potential days when exceptional events may be responsible for ozone exceedances.

1.4 Recommendations

We recommend using the lessons learned in this study to improve the 2019 NRTEEM system. We provide the following recommendations to improve the usefulness of the modeling system by:

- Using the latest available versions of WRF and CAMx model code

- Using new emissions inventory from TCEQ if available
- Working with TCEQ to refine the Mexico emission inventory
- Improving treatment of stratospheric influence by counting influx through lateral boundaries above tropopause height (in addition to influx through top boundary) and adding more vertical layers near the tropopause
- Continuing to investigate sensitivity tests around the base case such as alternate sources of boundary condition
- Performing additional LI analyses for different regions including San Antonio with input from TCEQ

In addition to the suggestions above to improve the modeling system, we provide the following recommendations to make the modeling website better:

- Using a dedicated machine for hosting NRTEEM website
- Other improvements proposed by TCEQ

2.0 BACKGROUND

The purpose of this study is to implement and refine the photochemical grid model system used by the TCEQ for the State Implementation Plan (SIP) planning by modelling ozone in a NRT mode in order to identify potential exceptional event impacts. We evaluate ozone impacts from fires, Mexican anthropogenic emissions and stratospheric ozone and evaluate model performance statistics to measure the impacts of different model configurations and identify areas for improvement.

The NRTEEM system was adapted from the FIM system. Lessons learned from the FIM system and sensitivity simulations run in previous NRT projects have aided us in our design of the 2018 base model run configuration, in terms of performance and reliability.

We presented a complete overview of the 2013 project in Johnson et al. (2013). We found that the ozone model performed well when high ozone was observed. A general lack of cloud cover and stagnant conditions from WRF meteorology led to ozone over-predictions when observed ozone was low to moderate. Johnson et al. (2015) provides a summary of the 2014 project. The 2014 modeling improved overall ozone bias and error relative to the 2013 modeling, despite much lower observed ozone overall. In the 2015 project, we found improvement in reducing persistent positive ozone bias and discovered that choice of analysis fields in WRF has a substantial impact on ozone (Johnson et al., 2016a). Finally, the 2016 project found further improvement in reducing positive ozone bias, though background ozone was still consistently overestimated in Houston and, to a lesser extent, Dallas. We constructed an ensemble model by averaging together results from five simulations to investigate whether a forecast ensemble could demonstrate greater skill than the individual simulations that go into the ensemble. Lack of sufficient ensemble member diversity hampered our ability to produce a useful ensemble prediction (Johnson et al., 2016b). The 2017 Fire Impact Modeling (FIM) system demonstrated usefulness by identifying potential days when exceptional events may be responsible for ozone exceedances (Johnson et al., 2017).

This report describes the various components of the development of the NRTEEM system, and presents an evaluation of potential exceptional event impacts and other model results.

First, we detail our modeling cycle in Section 3.1, including information about run schedule and data sources used. We then specify our WRF and CAMx configurations in Section 3.3, and describe our sensitivity tests and why they were selected in Section 3.4. Next, we present qualitative and quantitative analyses of model results in Section 4, including relative performance of the base case versus sensitivity tests and potential exceptional events. Finally, in Section 5 we discuss various recommendations as improvements to the 2019 NRTEEM system.

3.0 NEAR-REAL TIME EXCEPTIONAL EVENT MODELING SYSTEM

This section describes the components of the NRTEEM system. We detail our modeling cycle, including information about run schedule and data sources used. We then describe our WRF and CAMx configurations, CAMx sensitivity tests and finally, features of the NRTEEM website.

3.1 Modeling Cycle

We utilize the modeling system as developed for the 2017 FIM project which was developed from the 2013-2016 NRT projects. Ramboll runs the NRTEEM system for 24 simulation hours (1 full day from midnight to midnight in CST). The term initialization is used because the meteorological simulation is started from initial conditions at this time. Ramboll uses 0.25 degree Global Forecasting System (GFS) data assimilation system (GDAS) analysis data (Ek et al., 2014) as initial conditions for the WRF meteorological model. This GDAS data is also used for boundary conditions and data assimilation. Because the NRTEEM system runs a modeling cycle with at least a 1-day lag, observations and analyses are available to the WRF model for the entire modeling cycle and therefore no GFS forecast data needs to be used. We are not able to utilize the NAM (North American Mesoscale) data assimilation system (NDAS) analysis data because it does not cover our expanded 36 km domain (shown in Figure 3-1) used in the NRTEEM system.

Model images were uploaded to the NRTEEM website as model results were processed. Images for the entire modeling period (March 1 – June 30, 2018) were generated for:

- Hourly ozone, NO, NOx, CO concentrations
- Daily maximum 1-hour and 8-hour average ozone concentrations
- Hourly 2-m temperature, PBL height, wind speed, wind vectors, incoming solar radiation

Users can select images for any modeling cycle for the base case and all sensitivity simulations.

As developed for the 2016 NRT project, Ramboll delivered zoom-able, interactive statistics charts to the site which use observations from the TCEQ Continuous Air Monitoring Station (CAMS) and other monitors in Arkansas, Oklahoma and Louisiana. Normalized Mean Bias (NMB), Normalized Mean Error (NME) and correlation coefficient (r) statistics are available for ozone, NO, NOx, CO, 2-meter temperature, wind speed, wind direction and solar radiation. New pages displaying global concentration plots and satellite imagery have been newly developed for NRTEEM and are described in Section 3.5.

3.2 Modeling Domains

Figure 3-1 presents the 36/12/4 km WRF and CAMx modeling domains used for the NRTEEM system. The expanded 36 km WRF and CAMx modeling domains include all of Mexico, the Yucatan Peninsula, Belize and much of Guatemala. The 12/4 km domains are the TCEQ SIP domains, which have been used for other modeling efforts performed by Ramboll. The vertical layer mapping table from lowest 38 layers (43 total) in WRF to 28 layers in CAMx, is presented

in Figure 3-2. As with the modeling domains, this layer mapping is from the TCEQ SIP modeling and other recent modeling work performed by Ramboll.

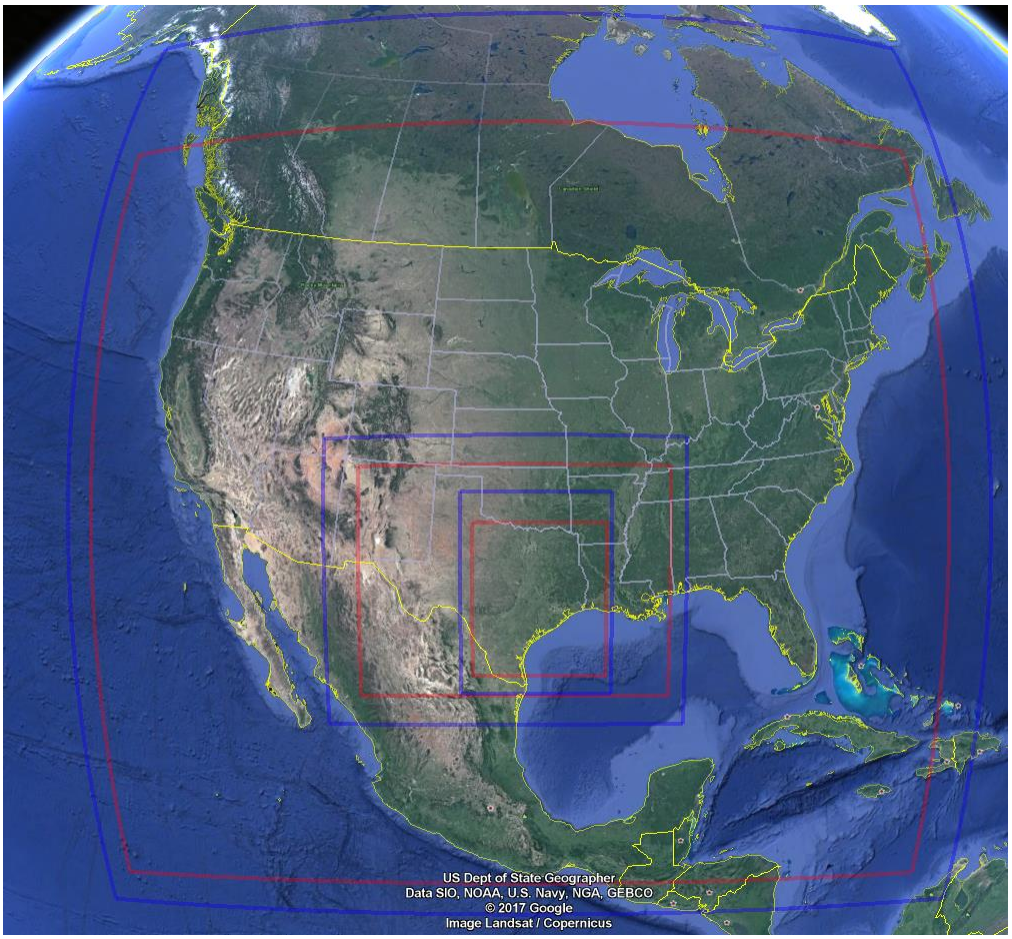

WRF Domain	Range (km)		Number of Cells		Cell Size (km)	
	Easting	Northing	Easting	Northing	Easting	Northing
North America Domain	(-2916,2916)	(-3024,3024)	163	169	36	36
South US Domain	(-1188,900)	(-1800,-144)	175	139	12	12
Texas Domain	(-396,468)	(-1620,-468)	217	289	4	4
CAMx Domain	**Range (km)**		**Number of Cells**		**Cell Size (km)**	
	Easting	**Northing**	**Easting**	**Northing**	**Easting**	**Northing**
RPO 36km Domain	(-2736,2592)	(-2808,1944)	148	132	36	36
Texas 12km Domain	(-984,804)	(-1632,-312)	149	110	12	12
Texas 4km Domain	(-328,436)	(-1516,-644)	191	218	4	4

Figure 3-1. WRF and CAMx 36/12/4 km modeling domains as used in the FIM system.

Vertical Layer Structure

Corresponding WRF Layer	Layer Top (m AGL)	CAMx Layer	Layer Center (m AGL)	Thickness (m)
38	15179.1	28	13637.9	3082.5
36	12096.6	27	10631.6	2930.0
32	9166.6	26	8063.8	2205.7
29	6960.9	25	6398.4	1125.0
27	5835.9	24	5367.0	937.9
25	4898.0	23	4502.2	791.6
23	4106.4	22	3739.9	733.0
21	3373.5	21	3199.9	347.2
20	3026.3	20	2858.3	335.9
19	2690.4	19	2528.3	324.3
18	2366.1	18	2234.7	262.8
17	2103.3	17	1975.2	256.2
16	1847.2	16	1722.2	249.9
15	1597.3	15	1475.3	243.9
14	1353.4	14	1281.6	143.6
13	1209.8	13	1139.0	141.6
12	1068.2	12	998.3	139.7
11	928.5	11	859.5	137.8
10	790.6	10	745.2	90.9
9	699.7	9	654.7	90.1
8	609.7	8	565.0	89.3
7	520.3	7	476.1	88.5
6	431.8	6	387.9	87.8
5	344.0	5	300.5	87.1
4	256.9	4	213.8	86.3
3	170.6	3	127.8	85.6
2	85.0	2	59.4	51.0
1	33.9	1	17.0	33.9

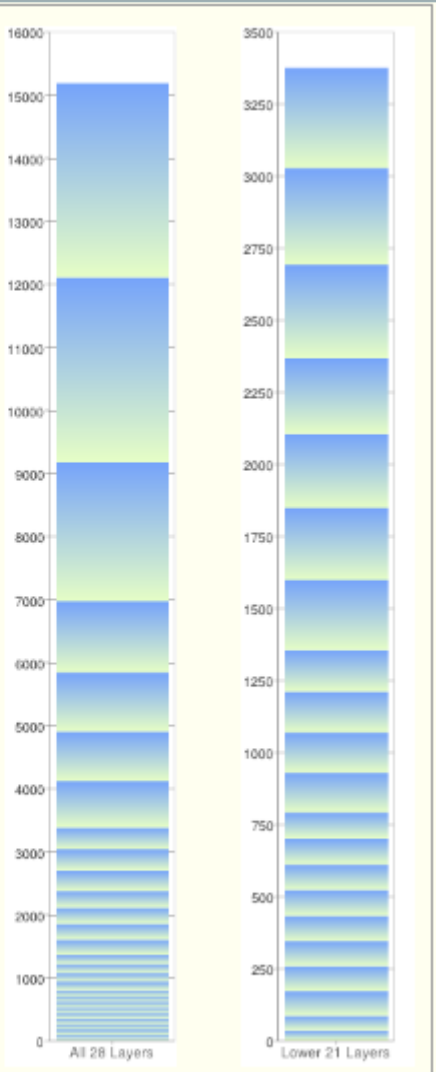

AGL - Above Ground Level.

Figure 3-2. CAMx Model Layer Structure. TCEQ figure from http://www.tceq.texas.gov/airquality/airmod/rider8/modeling/domain.

3.3 Models, Configurations, and Data

We present a general overview of the input/output and processing streams for the NRTEEM system in Figure 3-3. A description of the inputs used and configuration of the WRF and CAMx models follows.

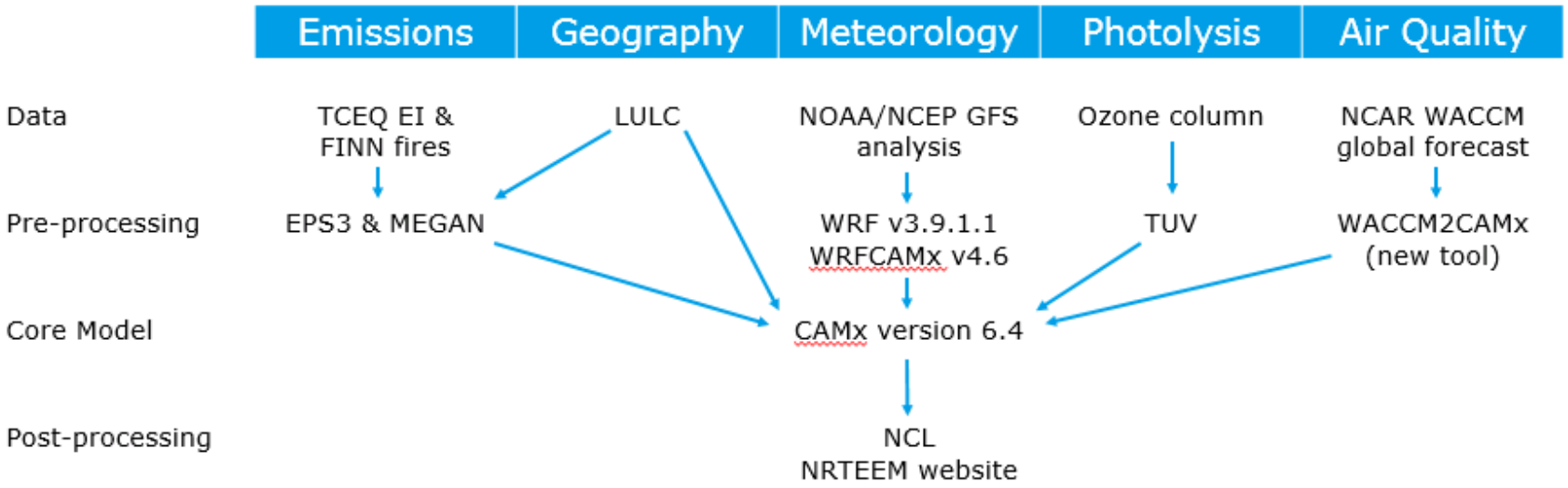

Figure 3-3. CAMx flow chart detailing input/output and processing streams for the NRTEEM system.

3.3.1 Meteorology

We are utilizing WRF v3.9.1.1 (released August 2017; Skamarock et al., 2008) for the NRTEEM system, the latest version of the model available at the start of the project. We provide the WRF physics options in Table 3-1. This configuration is similar to that used for the TCEQ SIP modeling. We are using MPI (Message Passing Interface) for our WRF simulations, utilizing 28 cores. Previous experience with WRF guided us to this configuration, as performance gains from either increasing the number of cores or using a hybrid MPI/OMP (Open Multi-Processing) approach were found to be minimal for WRF, in contrast to CAMx.

Table 3-1. WRF v3.9.1.1 physics options used in the NRT ozone modeling system.

WRF Physics Option	Option Selected	Notes
Microphysics	WRF Single-Moment 6-class (WSM6)	A scheme with ice, snow and graupel processes suitable for high-resolution simulations.
Longwave Radiation	RRTMG	Rapid Radiative Transfer Model. An accurate scheme using look-up tables for efficiency. Accounts for multiple bands, and microphysics species.
Shortwave Radiation	RRTMG	Rapid Radiative Transfer Model. An accurate scheme using look-up tables for efficiency. Accounts for multiple bands, and microphysics species.
Surface Layer Physics	MM5 similarity	Based on Monin-Obukhov with Carslon-Boland viscous sub-layer and standard similarity functions from look-up tables
LSM	Noah	NCEP/NCAR land surface model with soil temperature and moisture in four layers, fractional snow cover and frozen soil physics.
PBL scheme	Yonsei University (YSU)	Non-local-K scheme with explicit entrainment layer and parabolic K profile in unstable mixed layer
Cumulus parameterization	MSKF WRF	Multi-Scale Kain-Fritsch (MSKF) cumulus parameterization includes feedback of subgrid cloud information to the radiation schemes.

3.3.2 CAMx Configuration

Ramboll selected CAMx version 6.40 (released December 2016; Ramboll 2016) for the NRTEEM system, the latest version of the model at the start of the project. This is same CAMx version used in the 2017 FIM system.

Table 3-2 gives the CAMx configuration options that are currently in use. We utilize a hybrid MPI/OMP configuration for CAMx. We determined from model benchmarking that 14 MPI slice x 4 OMP thread setup was the optimum configuration for this application.

Table 3-2. CAMx v6.40 options used for the NRTEEM system.

Science Options	Configuration	Comments
Model Code	CAMx Version 6.40	Released December 2016
Time Zone	Central Standard Time (CST)	
Vertical Layers	28 layers (model top approximately 100 mb)	Lowest 21 CAMx layers match lowest 21 WRF layers
Chemistry Gas Phase Chemistry	CB6r4	CB6r4 combines a condensed set of reactions involving ocean-borne inorganic iodine from the CB6r2h full halogen mechanism with the temperature- and pressure-dependent organic nitrate branching ratio introduced in CB6r3.
Aerosol Chemistry	None	Primary PM smoke tracers from NRT FINN fire emissions are inert
Plume-in-Grid	None	Turned off; run-time consideration for FIM modeling
Photolysis Rate Adjustment	In-line TUV	Adjust photolysis rates for each grid cell to account for clouds and primary PM smoke tracers. Certain photolysis rates adjusted for temperature and pressure.
Meteorological Processor Subgrid Cloud Diagnosis	WRFCAMx CMAQ-based	Sub-grid clouds diagnosed from WRF grid-resolved thermodynamic properties.
Horizontal and Vertical Transport Eddy Diffusivity Scheme Diffusivity Lower Limit	 K-Theory Kz_min = 0.1 m^2/s	Vertical diffusivity (Kv) fields patched to enhance mixing: 1. over urban areas in lowest 100 m (OB70 or "Kv100" patch) 2. in areas where convection is present, by extending the daytime PBL Kv profile through capping cloud tops (cloud patch)
Dry Deposition	Wesely (1989)	Utilizes 11 landuse categories and does not use LAI
Numerical schemes Gas Phase Chemistry Solver Horizontal Advection Scheme	 Euler Backward Iterative (EBI) Piecewise Parabolic Method (PPM) scheme	As used in TCEQ SIP modeling

We are using the following CAMx inputs for the NRTEEM system:

- Initial conditions and boundary conditions extracted from NRT Whole Atmosphere Community Climate Model (WACCM) chemical forecasts from NCAR (https://www.acom.ucar.edu/waccm/forecast/). Chemical forecasts are run each day using WACCM, driven by GEOS-5 meteorology and including the standard (100 species) chemical mechanism.
- Initial conditions were extracted only for the initialization of the February 14, 2018 modeling cycle; subsequent cycles restarted from previous cycle.
- For the boundary conditions, NRT WACCM chemical forecasts were not available for March 17-28, so chemical forecasts averaged for the preceding week (March 11-16) were used to extract boundary conditions for these missing days.
- 2017 day-of-week specific anthropogenic emissions inventory provided by the TCEQ
- Month-specific elevated point source emissions provided by the TCEQ
- 2010 EDGAR global 0.1 degree emissions based on EPA's HTAP emissions modeling platform used outside TCEQ 36 km domain.
- MEGAN v2.10 biogenic emissions using current WRF modeling cycle meteorology with:
  - Isoprene emission factors incorporate aircraft data (EFvA2015) as in (Yu et al., 2015)
  - All non-isoprene species use EFvE2015 emission factors
  - PFTv2015 includes corn crop fix for plant functional type
  - Leaf Area Index (LAI) inputs include urban enhancements in Texas (Kota et al., 2015)
- WRFCAMx v4.6 using YSU Kv methodology
- Kv landuse patch up to 100 m and Kv cloud patch applied
- O3MAP: 2016 monthly averages from 1 degree TOMS satellite ozone column data
- Photolysis rates files generated using O3MAP 2016 monthly averages
- Land use / land cover inputs from TCEQ's HGB SIP modeling database; MODIS IGBP (International Geosphere Biosphere Programme) land use / land cover used outside TCEQ 36 km

3.3.3 Update to NRT FINN Fire Emissions

For the NRTEEM project, we re-mapped the FINN fire emissions species to simulate more realistic (rapid) NOx to NOy conversion. This approach applies vegetation type-dependent scale factors (see Table 3-3) and was obtained from the 2015 Texas Air Quality Research Program (AQRP) Fires project (McDonald-Buller et al., 2015).

Table 3-3. NOx-to-NOy FINN fire emissions species mapping factors by vegetation type.

		Vegetation Type Scale Factor		
Species	**FINN**	**A**	**B**	**C**
NO	NOx	0.000	0.000	0.000
NO2	NOx	0.736	0.421	0.451
PAN	NOx	0.056	0.144	0.128
PANX	NOx	0.008	0.104	0.072
NTR2	NOx	0.020	0.050	0.050
HNO3	NOx	0.180	0.280	0.300

A: Grasslands/Savanna/Woody Savanna/Shrublands/Croplands
B: Tropical Forest
C: Temperate Forest

To evaluate the impact of the NOx-to-NOy conversion, we developed a sensitivity simulation with the re-speciated FINN emissions (NOx2NOy) for the April 28, 2017 Mexico/Central America biomass burning episode that we evaluated for the 2017 FIM project (Johnson et al., 2017). Figure 3-4 shows the extent of the smoke plume ($PM_{2.5}$ tracer in left panel), base model NOx concentrations (middle) and NOx impacts (NOx2NOy-base) from the new FINN fire emissions. NOx concentrations decrease from the re-speciation. The magnitude of this impact is over 50 ppb where fires are burning. This finding is consistent with the AQRP Fires study (McDonald-Buller et al., 2015).

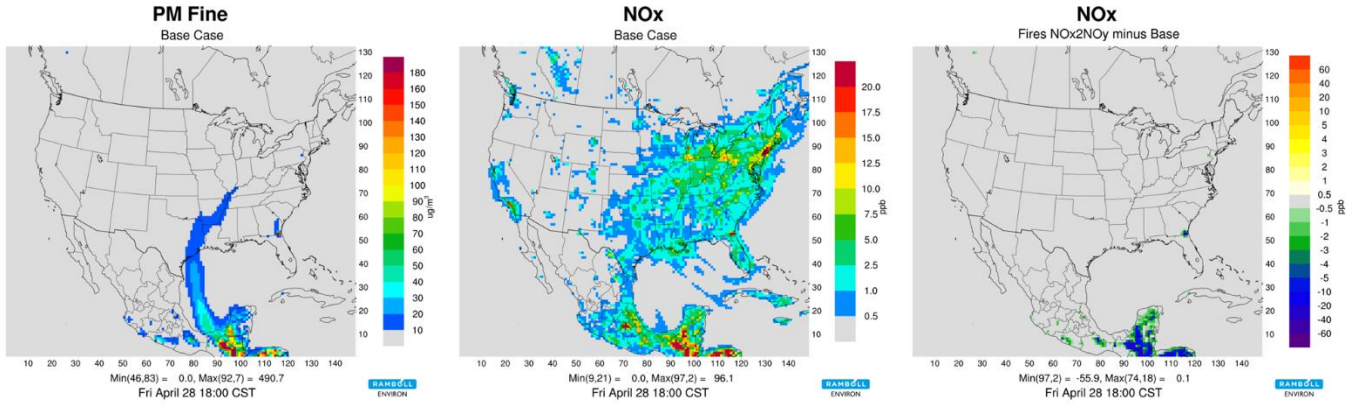

Figure 3-4. Hourly $PM_{2.5}$ smoke tracer (left), NOx (middle) and NOx difference (NOx2NOy-base) concentrations for April 28, 2017 18:00 CST.

Next, we evaluate ozone impacts from the FINN fire emissions re-speciation in Figure 3-5. The left panel is the same as in Figure 3-4. The middle and right panels are similar to Figure 3-4 but show ozone concentrations instead of NOx. We find that the lower NOx emissions lead to ozone decreases in the smoke plume. The magnitude of this impact is up to 5 ppb in East Texas. Additionally, we find ozone increases in areas where NOx was titrating ozone in the base run. This finding is also consistent with the AQRP Fires study (McDonald-Buller et al., 2015).

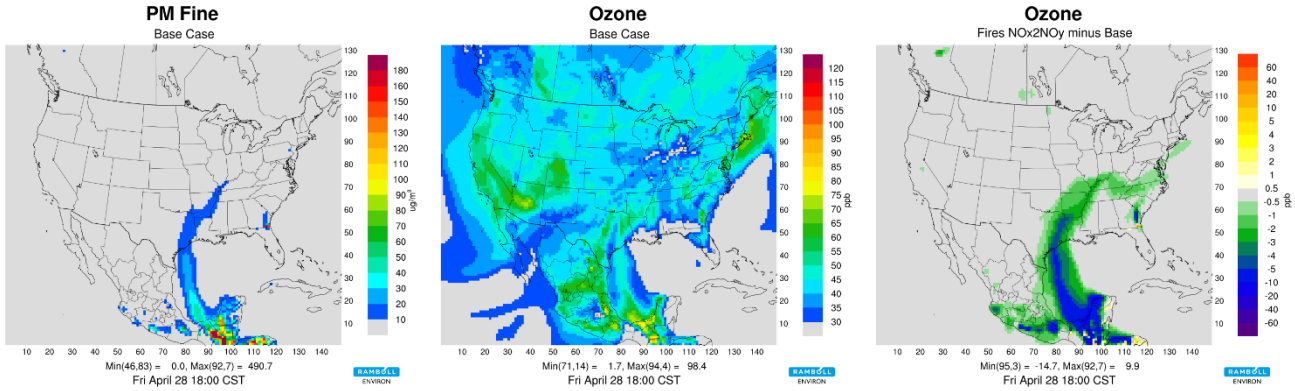

Figure 3-5. Hourly $PM_{2.5}$ smoke tracer (left), Ozone (middle) and Ozone difference (NOx2NOy-base) concentrations for April 28, 2017 18:00 CST.

3.4 Sensitivity Tests

Table 3-4 describes the sensitivity simulations used in the 2018 NRTEEM system. CAMx sensitivity simulations were run in parallel with the "base case" simulation. We selected the sensitivity tests to determine the impact of fires (No Fires), Mexico anthropogenic emissions (No Mexico Anthro) and stratospheric ozone intrusions (Stratospheric Ozone) on Texas ozone.

The No Fires, No Mexico Anthro and Stratospheric Ozone simulations were run for the entire modeling period of the Base simulation, March – June 2018. The Zhang and Zhang Mod simulations were run for April – June 2018.

Table 3-4. CAMx sensitivity simulations utilized in the NRTEEM system. The sensitivity tests in the last two rows were run for April – June 2018.

Sensitivity Simulation	Description
No Fires	Remove fires emissions. No inert aerosol tracers modeled.
No Mexico Anthro	Zero-out Mexico emissions from all anthropogenic sectors.
Stratospheric Ozone	Do not cap ozone top concentrations.
Zhang	Replace Wesely with Zhang dry deposition scheme.
Zhang Mod	Used modified version of Zhang scheme that adjusts surface resistances to improve ozone deposition in forested areas and over the ocean.

We developed a No Fires sensitivity simulation that removes NRT FINN fire emissions. This run was designed so that its ozone concentrations could be subtracted from the base simulation to calculate the ozone impact from wildfire emissions.

Next, we developed the No Mexico Anthro sensitivity which removed all anthropogenic emissions from Mexico. Biogenic and wildfire emissions within Mexico were included in this run. For this run, we applied a mask to all model grid cells covering Mexico and removed all anthropogenic emissions within those cells. We wanted to quantify how much ozone could be attributed to Mexico and determine if any substantial impacts occurred when observed ozone was high during the entire March – June 2018 modeling period.

The next sensitivity is Stratospheric Ozone. While the base model caps ozone top concentrations at 100 ppb, this sensitivity does not cap ozone top concentrations. Neither model caps ozone from the lateral boundaries.

Finally, we developed two new simulations to examine the impacts of dry deposition on ozone: Zhang and Zhang Mod. These two simulations cover April – June 2018. The Zhang simulation simply replaces the Wesely dry deposition scheme in the base model with the Zhang scheme. The Zhang Mod simulation changes surface resistances in forested areas (see Table 3-5) and over the ocean to alternative values that are within plausible ranges (after the ZHANG-$r_{s,min}$ sensitivity test of Wu et al. 2018) and will tend to increase ozone deposition.

Table 3-5. Minimum stomatal resistances (s m^{-1}) by land cover category for the Zhang and Zhang Mod simulations.

Land Cover Category	Zhang	Zhang Mod
Evergreen needleleaf trees	250	188
Evergreen broadleaf trees	150	113
Deciduous needleleaf trees	250	188
Deciduous broadleaf trees	150	113
Tropical broadleaf trees	150	113
Drought deciduous trees	250	188

3.5 New NRTEEM Website Features

Two new features were added to the NRTEEM website in 2018. New pages were constructed to display WACCM global air quality concentration plots and GOES-East satellite imagery.

3.5.1 WACCM Global Air Quality Concentration Plots

We constructed a new NRTEEM page to display WACCM global air quality concentrations (see Figure 3-6). The NRT WACCM concentrations were a new product from NCAR at the beginning of this project, so we wanted to have a simple way to observe WACCM output for the entire globe and track changes throughout the March – June 2018 period. The page shows WACCM global 6-hourly concentrations for ozone, NO2 and CO. The images can be animated for any time period selected via the date picker.

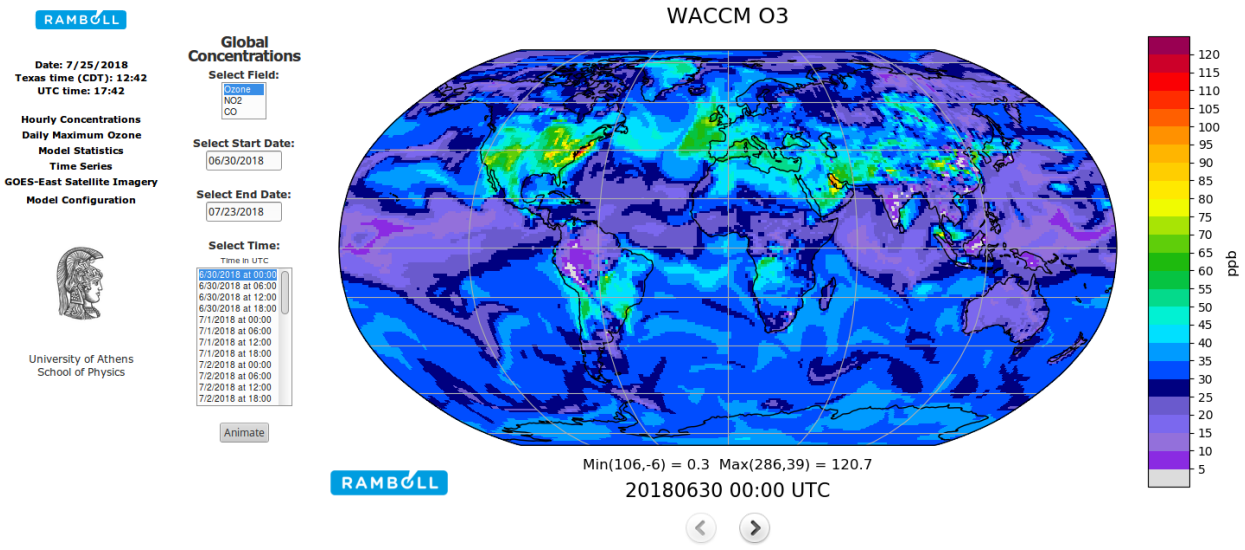

Figure 3-6. WACCM global concentrations page on the NRTEEM website.

3.5.2 GOES-East Satellite Imagery

Another recent addition to the NRTEEM website is the Geostationary Operational Environmental Satellite-East (GOES-East; formerly GOES-16) Satellite Imagery page (see Figure 3-7). The page allows selection of two different GOES-East Advanced Baseline Imager (ABI) wavelength products: 1) Red Visible (ABI Band 2: 0.64 um) and 2) Shortwave Infrared (ABI Band 7: 3.9 um). Each product is available at 15-minute intervals for each of the three modeling domain extents and each can be used to detect fires. Band 7 is used primarily to detect fire hotspots, while Band 2 is used to see smoke plumes. We use a modified version of the SatPy Python package[1] to generate imagery from the NRT GOES-East Level 1B radiances. As with the Global Concentrations page, the images can be animated for any time period selected via the date picker.

[1] https://github.com/pytroll/satpy

For Band 7, colder brightness temperatures are white (cold cloud tops) and warm land surfaces show up as dark grey or black. We applied a yellow-to-red color map for brightness temperatures greater than 60 C, intended as a way to identify larger/hotter fires. There are other phenomena that can generate brightness temperatures above this threshold including reflections from large solar arrays, intense solar heating of light colored desert landscapes and sunlight hitting the ocean at low sun angles near sunset. Resolution is about 2 km for this band (36 km imagery is about 6 km so that images can fit on the screen).

For Band 2, we only generate images for 7 AM-7 PM CST (visible bands are dark at night). These are greyscale images where clouds are white and smoke plumes show up as grey. The native resolution for this band is 500 m but the images become too large to view on the website for the domain extents at that resolution. The 36 km images are effectively 6 km resolution; 12 km are 2 km and 4 km are 1 km.

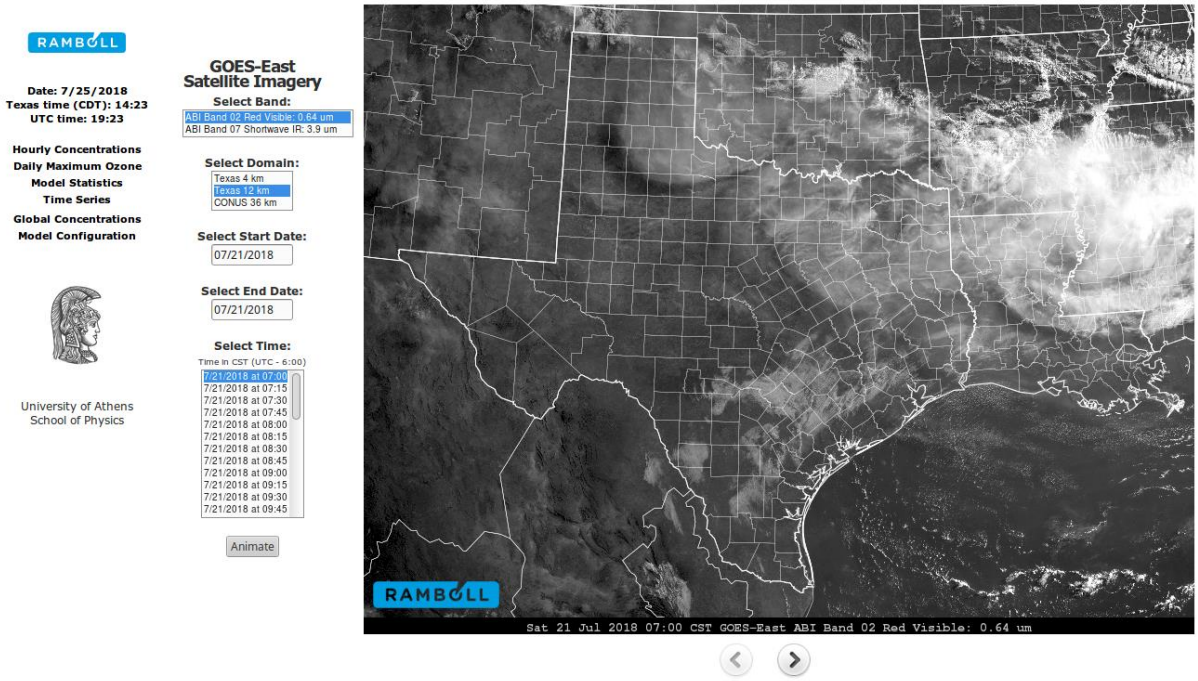

Figure 3-7. GOES-East satellite imagery page on the NRTEEM website.

Figure 3-8 shows example imagery for the shortwave IR Band 7 (left) and red visible Band 2 (right) for July 3, 2018 16:00 CST. This time was chosen to highlight the Surprise Fire in Palo Pinto County[2]. The fire hotspot is shown with yellow/orange pixels in the shortwave IR (left panel) which is collocated with the smoke plume in the red visible image (right panel).

[2] https://inciweb.nwcg.gov/incident/5890/

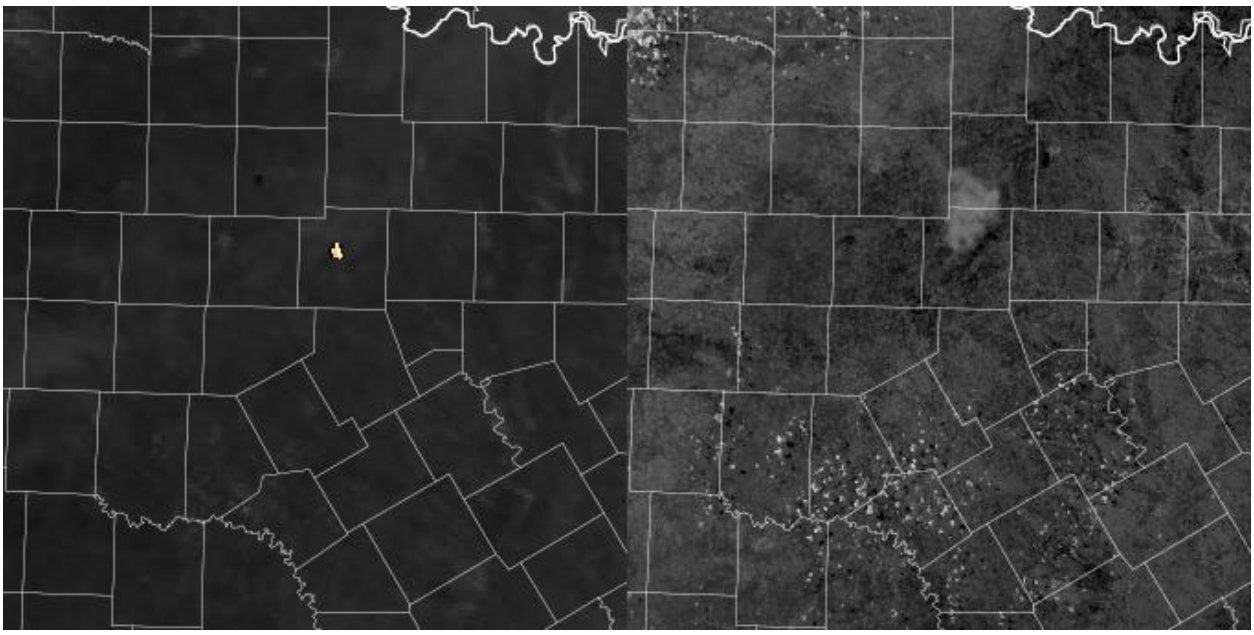

Figure 3-8. Example GOES-East satellite imagery (Shortwave IR Band 7: left; Red Visible Band 2: right) for July 3, 2018 16:00 CST zoomed in to show Surprise Fire in Palo Pinto County.

4.0 MODEL EVALUATION

This section presents quantitative and qualitative evaluations of WRF meteorological and CAMx ozone performance. The objective was to evaluate the Zhang simulations with respect to the base model to determine if ozone performance is substantially impacted by the changes to the deposition scheme.

In the sections below, we first provide results from the regional analysis of the base configuration, focusing on quantitative evaluation of the meteorological fields and ozone. Next, we provide an evaluation of the daily maximum 8-hour average (MDA8) ozone local increment (LI) analysis in Dallas and Houston. Then we examine the relationship between exceptional event impacts and model performance. Finally, we present case studies that examine potential exceptional events as modeled by the NRTEEM system.

4.1 WRF Meteorological Model Performance Evaluation

We evaluate WRF 2-m temperature, 2-m humidity and 10-m wind speed and direction using the Integrated Surface Data (ISD) data set ds3505.0, archived at the National Climatic Data Center (NCDC). Meteorological data from the TCEQ's CAMS are not used because some locations are known to have nearby obstructions that bias wind measurements from certain sectors (Johnson et al., 2015) and a systematic evaluation of which CAMS could be used for meteorological model performance evaluation is not available to us. For this report, we examine performance at ds3505.0 monitoring locations in Dallas, Houston-Galveston-Brazoria (HGB) and San Antonio (Figure 4-1).

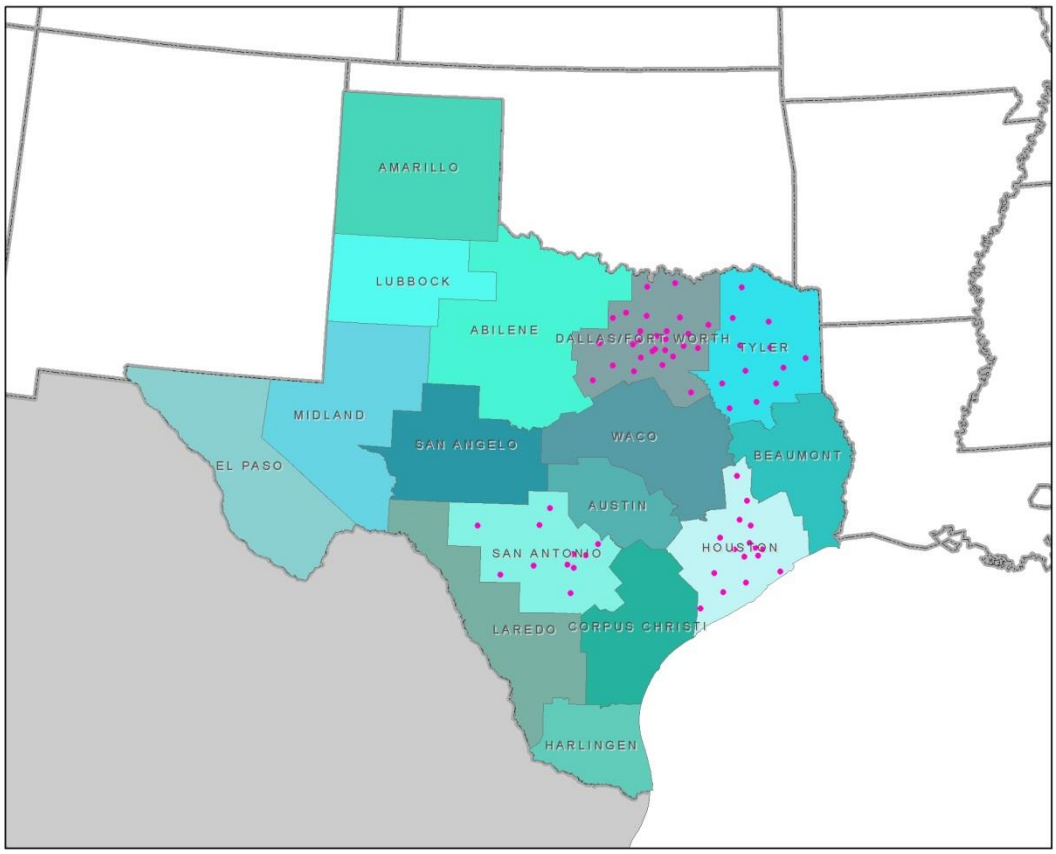

Figure 4-1. Map of ds3505.0 meteorological monitoring stations used in the WRF meteorological model performance evaluation.

Emery et al. (2001) derived and proposed a set of daily performance "benchmarks" for typical meteorological model performance. These standards were based upon the evaluation of about 30 MM5 and RAMS meteorological simulations of limited duration (multi-day episodes) in support of air quality modeling applications. These were primarily ozone model applications for cities in the eastern and Midwestern U.S. and Texas that were primarily simple (flat) terrain and simple (stationary high pressure causing stagnation) meteorological conditions. More recently these benchmarks have been used in meteorological modeling studies that include areas with complex terrain (McNally, 2009; ENVIRON and Alpine, 2012).

The purpose of the benchmarks is to help characterize how good or poor the results are relative to other model applications run for the U.S. In this section, the meteorological variables are compared to the benchmarks as an initial indication of the WRF performance. These benchmarks include model bias and error in temperature, wind direction and water vapor mixing ratio as well as the wind speed bias and Root Mean Squared Error (RMSE). The benchmarks for each parameter are as follows:

- Temperature Bias: less than or equal to ±0.5 °K; alternative of ≤±2.0 °K for complex conditions.
- Temperature Error: less than or equal to 2.0 °K; alternative of ≤2.5 °K for complex conditions.
- Mixing Ratio Bias: less than or equal to ±0.8 g/kg; alternative of ±1.0 g/kg for complex conditions.
- Mixing Ratio Error: less than or equal to 2.0 g/kg.
- Wind Direction Bias: less than or equal to ±10 degrees.
- Wind Direction Error: less than or equal to 30 degrees; alternative of 50 degrees for complex conditions.
- Wind Speed Bias: less than or equal to ±0.5 m/s; alternative of ±1.5 m/s for complex conditions.
- Wind Speed RMSE: less than or equal to 2 m/s; alternative of 2.5 m/s for complex conditions.

The equations for bias and error are given below, with the equation for the Root Mean Squared Error (RMSE) similar only being the square of the differences between the prediction and observation and a square root is taken of the entire quantity.

$$\text{Bias} = \frac{1}{N}\sum_{i=1}^{N}(P_i - O_i)$$

$$\text{Error} = \frac{1}{N}\sum_{i=1}^{N}\left|P_i - O_i\right|$$

The March 1 – June 30, 2018 average statistics for wind speed, wind direction, temperature and humidity for all ds3505.0 stations within Dallas are displayed graphically in Figure 4-2 using the so-called “soccerplot” displays. Soccerplots graph monthly average bias versus monthly average error. For wind speed, error is replaced with RMSE. Along with the results are the simple (plotted in black) and complex benchmark results (red). It is desirable to have the symbols lay inside the benchmark outline (i.e., score a goal in the soccer plot analogy).

We present soccerplot diagrams for Houston and San Antonio in Figure 4-3 and Figure 4-4, respectively. We find generally good performance with points falling within or close to the simple benchmark goals. Dallas shows the worst performance across the three regions, with values just outside the simple benchmarks in May for wind speed bias (RMSE > 2.0 m/s) and temperature (bias > 2.0 K). Overall, performance looks superior to that observed for 2017 FIM modeling.

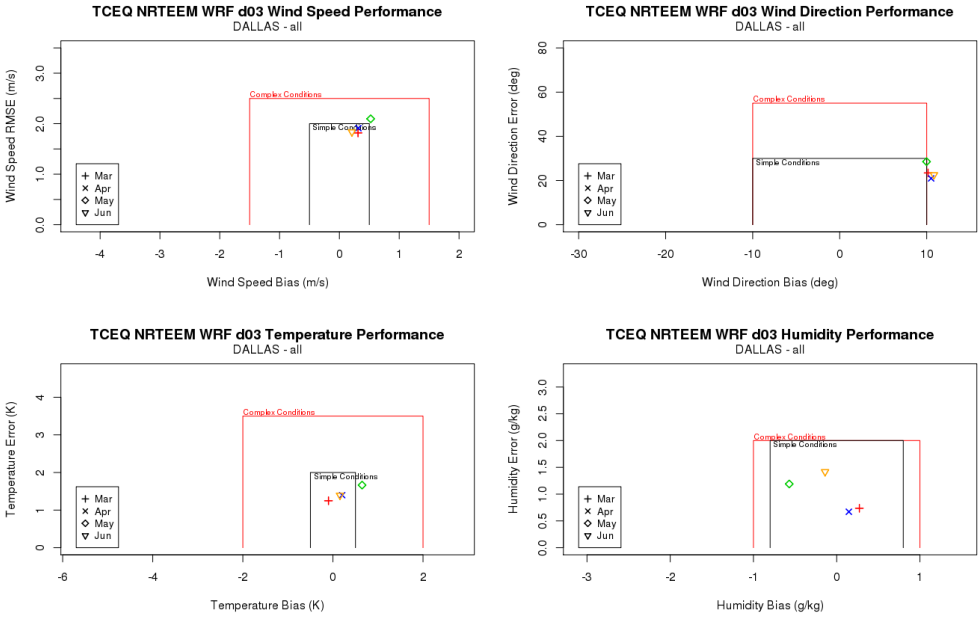

Figure 4-2. Soccer plots for wind speed (top left), wind direction (top right), temperature (bottom left) and humidity (bottom right) for all Dallas ds3505.0 monitoring stations covering March 1 – June 30, 2018.

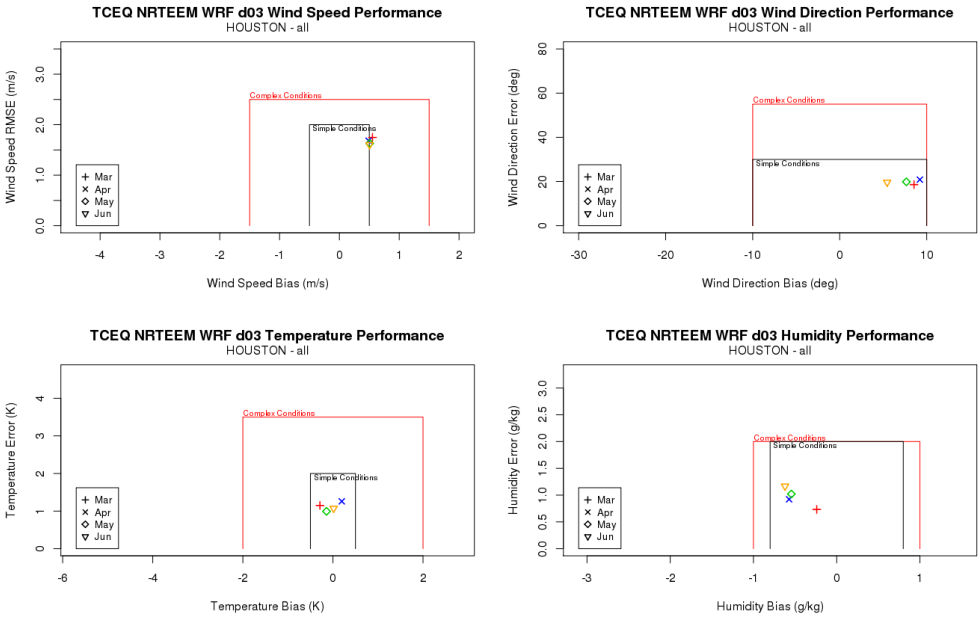

Figure 4-3. Soccer plots for wind speed (top left), wind direction (top right), temperature (bottom left) and humidity (bottom right) for all Houston ds3505.0 monitoring stations covering March 1 – June 30, 2018.

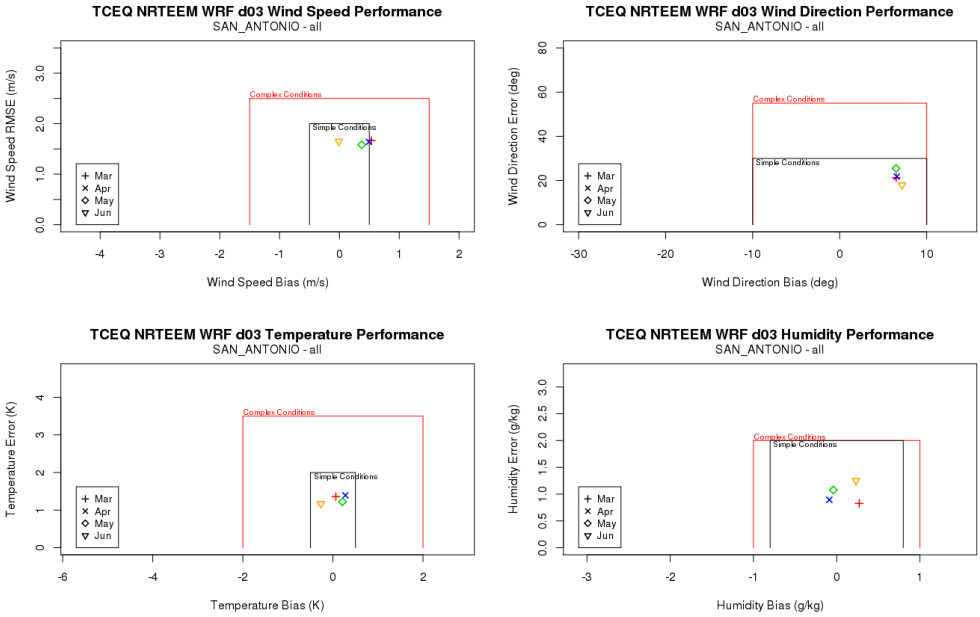

Figure 4-4. Soccer plots for wind speed (top left), wind direction (top right), temperature (bottom left) and humidity (bottom right) for all San Antonio ds3505.0 monitoring stations covering March 1 – June 30, 2018.

4.2 Operational Evaluation

We present the number of observed occurrences of MDA8 ozone above 70 ppb for the Dallas-Fort Worth, Houston-Galveston-Brazoria, El Paso and San Antonio regions in Figure 4-5. The plot suggests that March-June 2018 had more high ozone days than the previous two years. The exception is El Paso, where March-June 2018 had the same number of occurrences (10) as March-June 2017. The 2018 ozone season could have many more high ozone days which would change its ranking relative to previous ozone seasons.

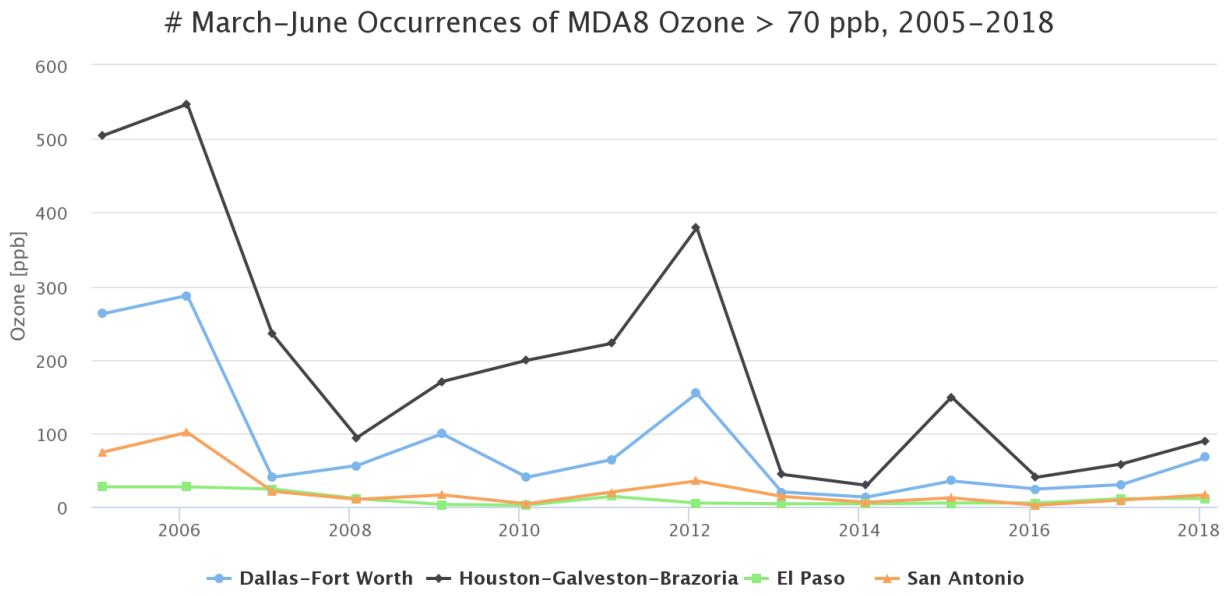

Figure 4-5. Number of occurrences of MDA8 ozone concentrations above 70 ppb during the months of March-June for the years 2005-2018 for the Dallas-Fort Worth, Houston-Galveston-Brazoria, El Paso and San Antonio metropolitan regions.

4.3 Model Performance Evaluation and Sensitivity Analysis

4.3.1 Case Study: April 23-29, 2018

During the week of April 23, 2018, Houston, Beaumont-Port Arthur, Dallas, Fort Worth, San Antonio, Killeen-Temple and Tyler ozone monitors all recorded MDA8 values exceeding 70 ppb (see Figure 4-6). On April 28 alone, 40 CAMS locations in these regions exceeded 70 ppb.

Metropolitan Area	One-Hour Averages >= 125 ppb			Eight-Hour Averages >= 71 ppb		
	Peak Value		High Days	Peak Value		High Days
	Date	ppb		Date	ppb	
Houston Includes: Harris County, TX; Montgomery County, TX	No averages at or above 125			04/28/2018	88	4
Dallas Includes: Collin County, TX; Dallas County, TX; Denton County, TX; Ellis County, TX; Hunt County, TX; Kaufman County, TX; Rockwall County, TX	No averages at or above 125			04/24/2018	81	2
Fort Worth-Arlington Includes: Hood County, TX; Johnson County, TX; Parker County, TX; Tarrant County, TX	No averages at or above 125			04/24/2018	77	2
San Antonio	No averages at or above 125			04/23/2018	77	3
Beaumont-Port Arthur Includes: Jefferson County, TX; Orange County, TX	No averages at or above 125			04/25/2018	77	2
Killeen-Temple	No averages at or above 125			04/28/2018	75	1
Galveston-Texas City	No averages at or above 125			04/24/2018	83	4
Brazoria	No averages at or above 125			04/24/2018	77	1
Tyler	No averages at or above 125			04/28/2018	73	1

Figure 4-6. TCEQ website graphic showing the peak ozone MDA8 value and number of days where MDA8 exceeded 70 ppb for all Texas regions where at least one monitor had an MDA8 value that exceeded 70 ppb.

To investigate how the base model simulation performed during this high ozone episode, we present daily 1-hour ozone statistics (NMB, NME and correlation coefficient) charts for the Houston region for April 23-29, 2018 in Figure 4-7. Numerical values for each statistic is shown for the day where observed ozone was highest in Houston, April 28. The base model shows excellent performance during the entire episode, especially on the highest day (NMB: +1.8%; NME: 13.8%).

In Figure 4-8, we present ozone time series (black dotted line: observations; blue line: base model) for April 23-29, 2018 at Lang (CAMS 408) in Houston. While the nighttime ozone minima are not well simulated, the model does an excellent job capturing midday peak ozone, especially on the day of highest observed ozone, April 28.

Finally, we present daily 1-hour ozone statistics (similar to Figure 4-7) for this high ozone episode for Beaumont-Port Arthur (Figure 4-9), Dallas-Fort Worth (Figure 4-10) and San Antonio (Figure 4-11). Each figure shows numerical values for the highest day of the episode (Apr 28 for BPA and DFW; Apr 23 for San Antonio). Again, we find excellent performance when observed ozone was highest.

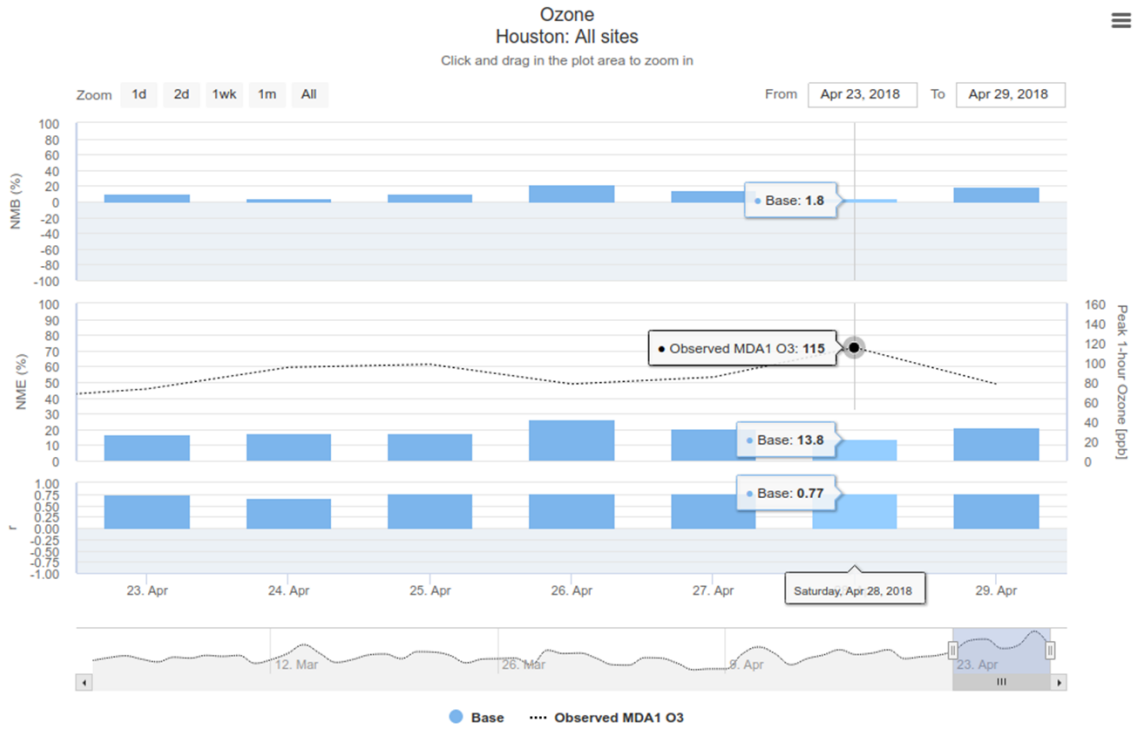

Figure 4-7. Houston model performance statistics for ozone (20 ppb cutoff) by area for the base simulation for April 23-29, 2018. Statistics shown for the highest day of the week, April 28.

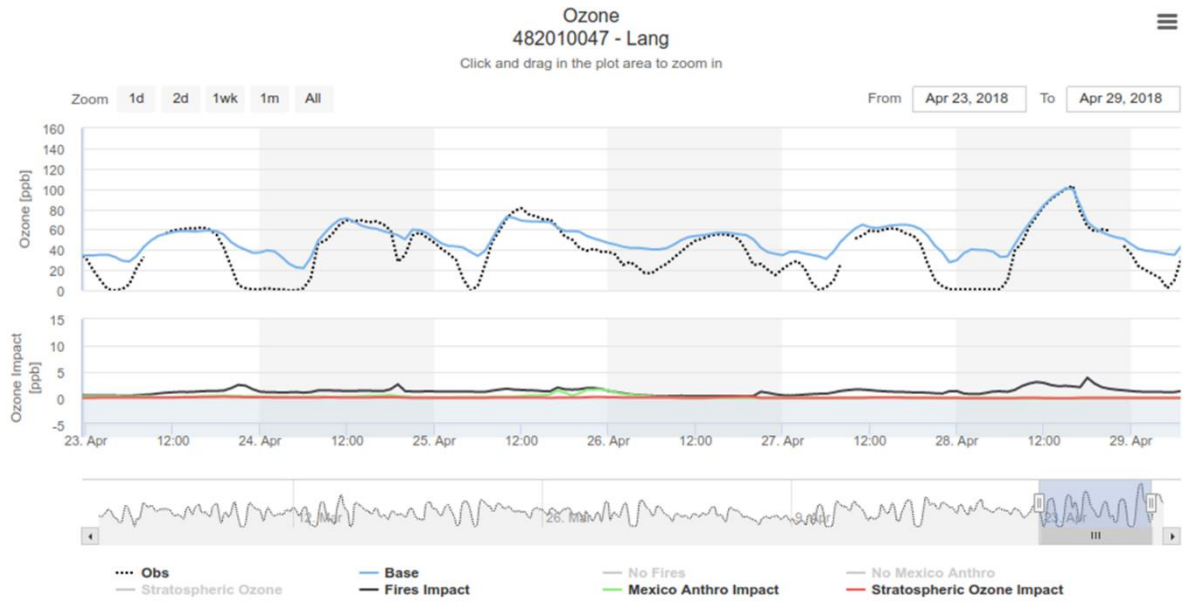

Figure 4-8. Observed (black dotted line), base model (blue) ozone time series for April 23-29, 2018 at Lang (CAMS 408) in Houston.

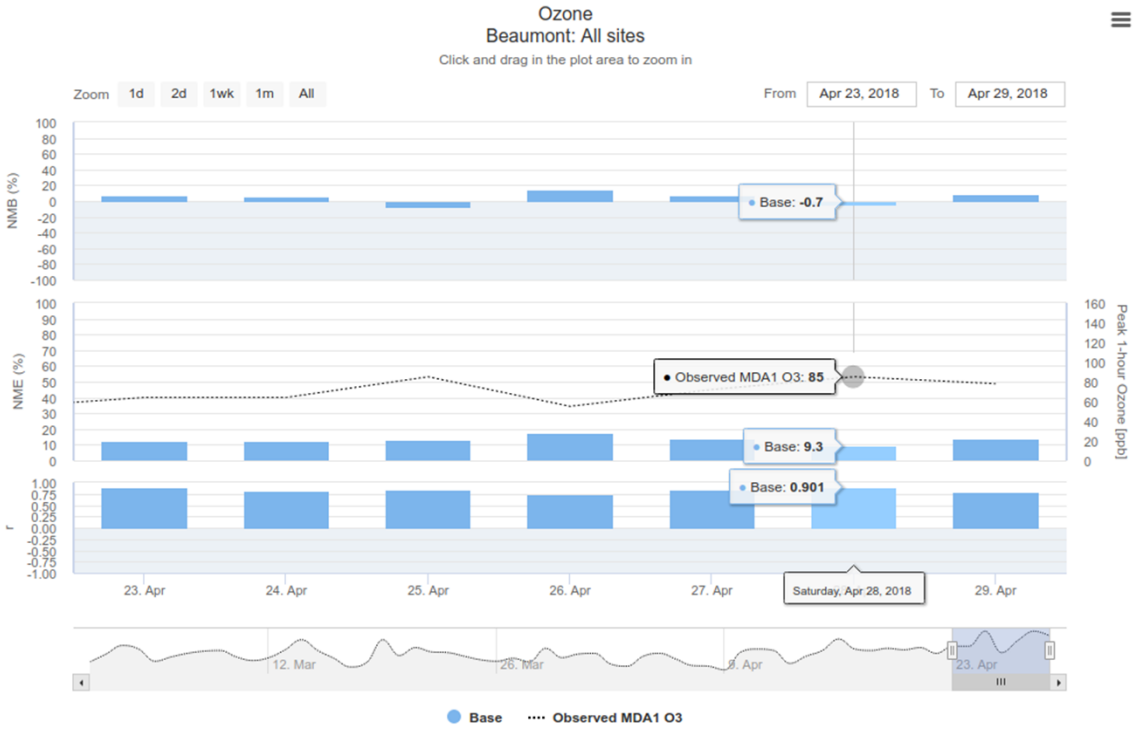

Figure 4-9. Beaumont-Port Arthur model performance statistics for ozone (20 ppb cutoff) by area for the base simulation for April 23-29, 2018. Statistics shown for the highest day of the week, April 28.

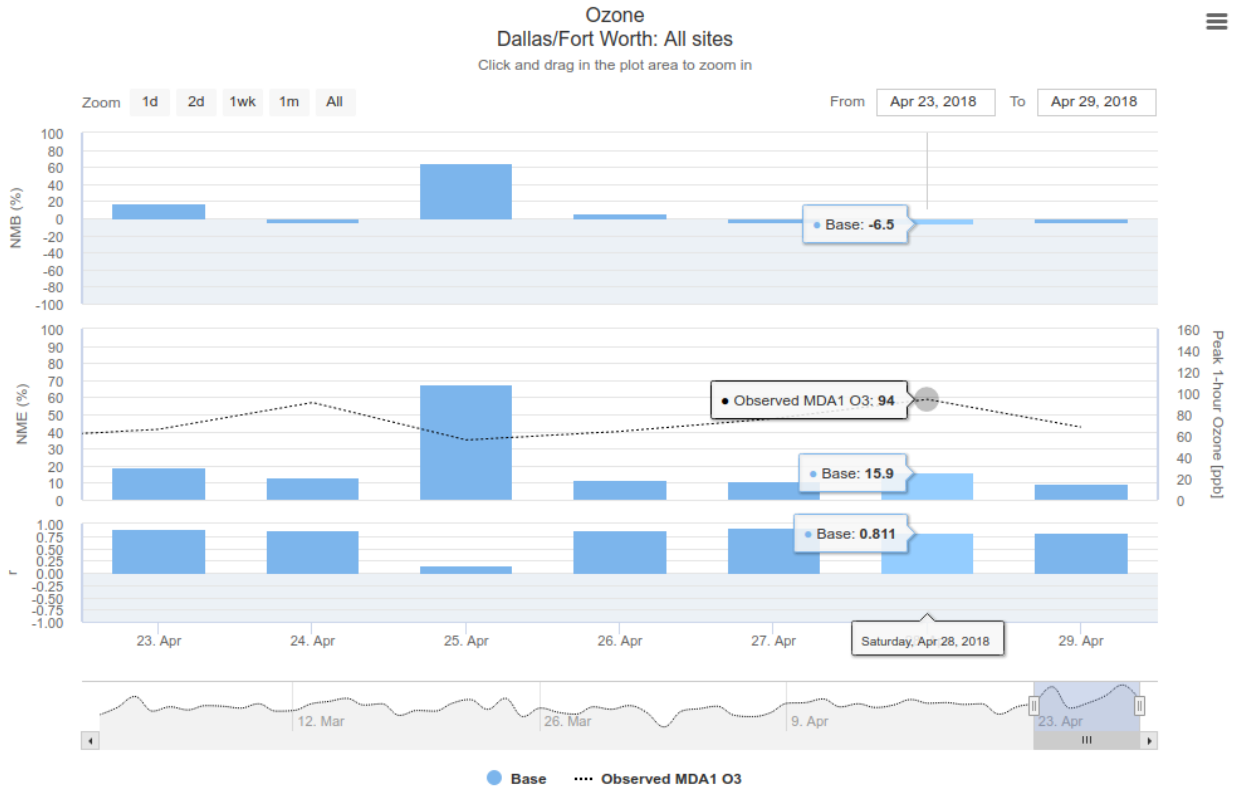

Figure 4-10. Dallas-Fort Worth model performance statistics for ozone (20 ppb cutoff) by area for the base simulation for April 23-29, 2018. Statistics shown for the highest day of the week, April 28.

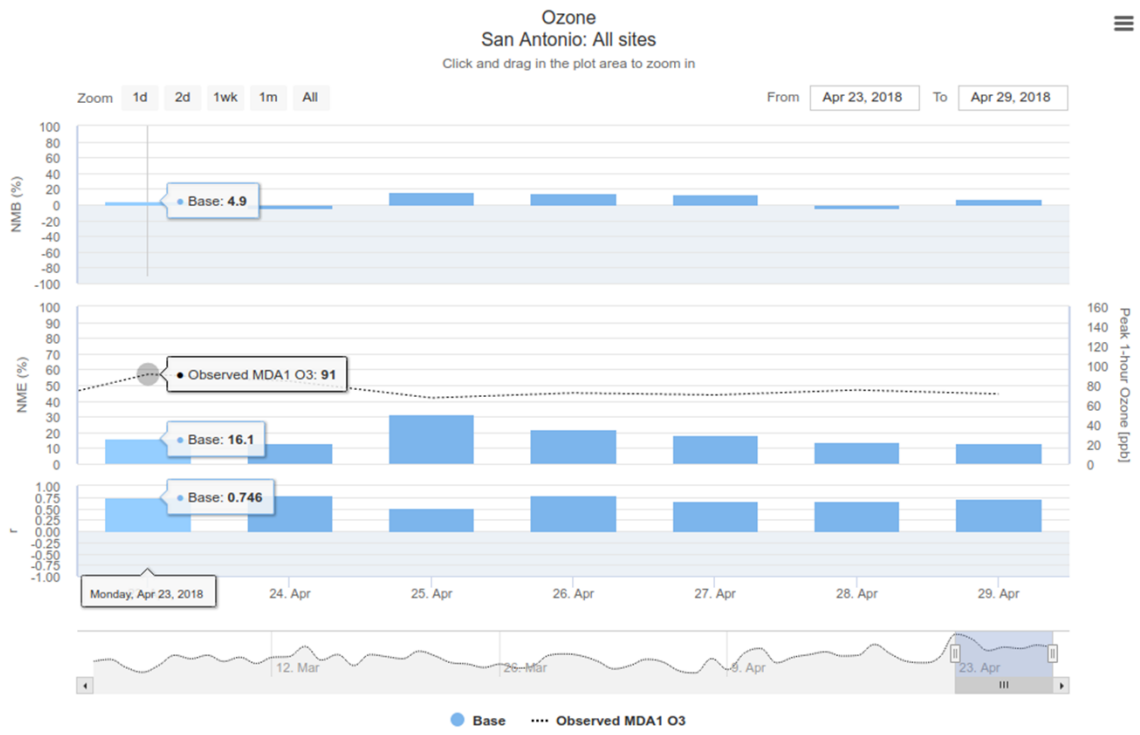

Figure 4-11. San Antonio model performance statistics for ozone (20 ppb cutoff) by area for the base simulation for April 23-29, 2018. Statistics shown for the highest day of the week, April 23.

4.3.2 Statistics

The CAMx NRTEEM website has been set up to compute model performance statistics for each CAMx run when observed data are available. Statistical metrics are computed for individual CAMS monitoring sites, major urban areas and the entire CAMS network.

The statistical metrics computed for CAMS monitoring locations are:

- Normalized Mean Bias (NMB)
  - $NMB = \frac{\sum_{i=1}^{N}(P_i - O_i)}{\sum_{i=1}^{N} O_i}$

    where P_i and O_i are the predicted and observed values (O_i,P_i) in a data pair and N is the number of observed/modeled data pairs.

- Normalized Mean Error (NME)
  - $NME = \frac{\sum_{i=1}^{N}|P_i - O_i|}{\sum_{i=1}^{N} O_i}$

- Correlation coefficient (r)

$$r = \frac{\sum_{i=1}^{N} P_i O_i - \frac{\left(\sum_{i=1}^{N} P_i\right)\left(\sum_{i=1}^{N} O_i\right)}{N}}{\sqrt{\left[\sum_{i=1}^{N} P_i^2 - \frac{\left(\sum_{i=1}^{N} P_i\right)^2}{N}\right]\left[\sum_{i=1}^{N} O_i^2 - \frac{\left(\sum_{i=1}^{N} O_i\right)^2}{N}\right]}}$$

Statistical metrics were computed for:

- Hourly ozone, NO, NOx and CO
- Hourly temperature, wind speed, wind direction, total solar radiation

A 20 ppb threshold was applied to observed ozone concentrations; thresholds of 1 mph and 10 Watts/m^2 were employed for wind speed and solar radiation, respectively. We note that because wind direction is an angular measurement, we replace NMB and NME with mean bias (MB) and mean error (ME), respectively.

We evaluated ozone model performance for the base and Zhang simulations for the following modeling period, April 1 through June 30, 2018.

4.3.3 1-Hour Ozone Statistical Evaluation

We present 1-hour ozone statistics across all Dallas CAMS for the base model in Figure 4-12. Similar plots for Houston and San Antonio are found in Figure 4-13 and Figure 4-14, respectively. We exclude the Zhang and Zhang Mod results for clarity. Similar figures are available on the NRTEEM website with interactive selection of date, region/site and model simulation. We observe the poorest performance (high positive bias) when ozone is relatively low (1-hour peak ozone below about 50 ppb; see April 2 in Figure 4-12 for an example). The base model performs very well during several high ozone days/episodes, including April 23-29 and May 5-10, 2018.

In general, the Zhang simulation results in higher ozone concentrations (due to lower ozone deposition compared to the Wesely deposition scheme used in the base model). Therefore, when the base model underestimates ozone, the Zhang simulation tends to improve performance. The Zhang Mod simulation results in lower ozone concentrations compared to Zhang, which results in performance similar to the base model.

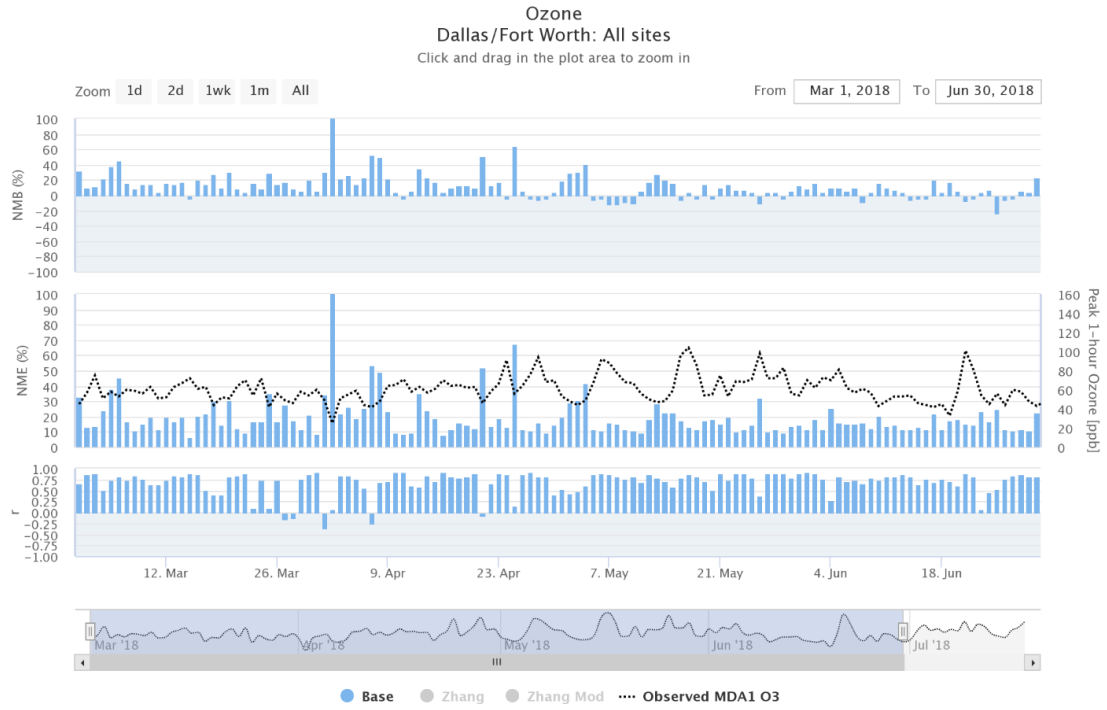

Figure 4-12. Dallas model performance statistics for ozone (20 ppb cutoff) by area for the base simulation for March 1 – June 30, 2018.

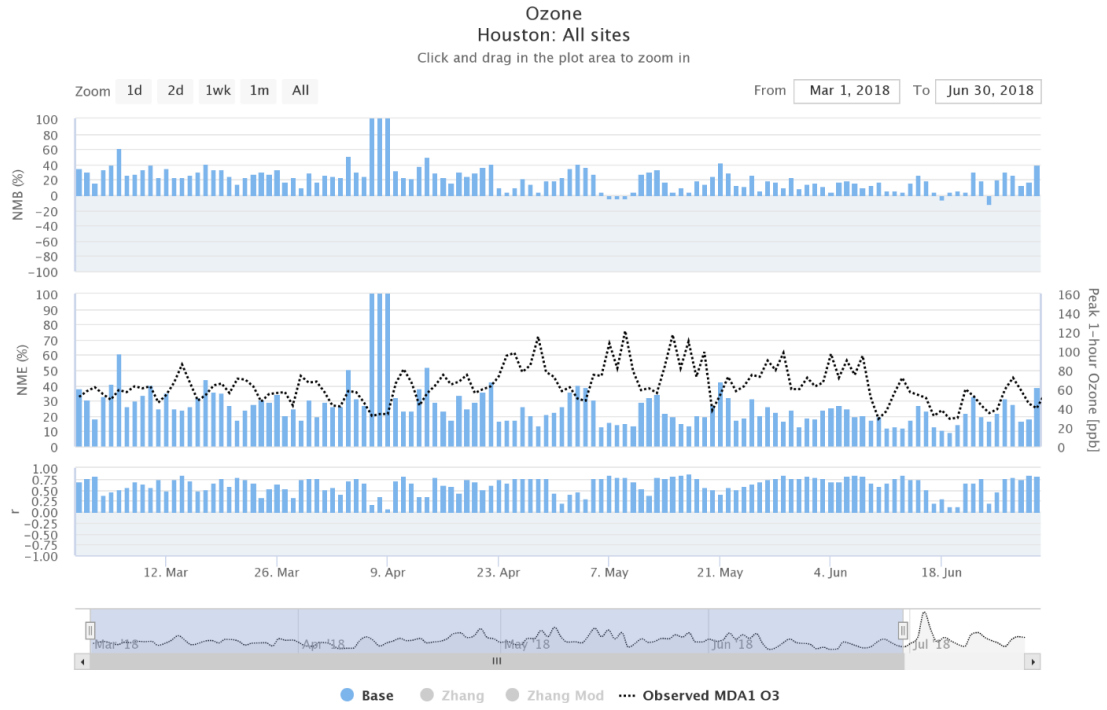

Figure 4-13. Houston model performance statistics for ozone (20 ppb cutoff) by area for the base simulation for March 1 - June 30, 2018.

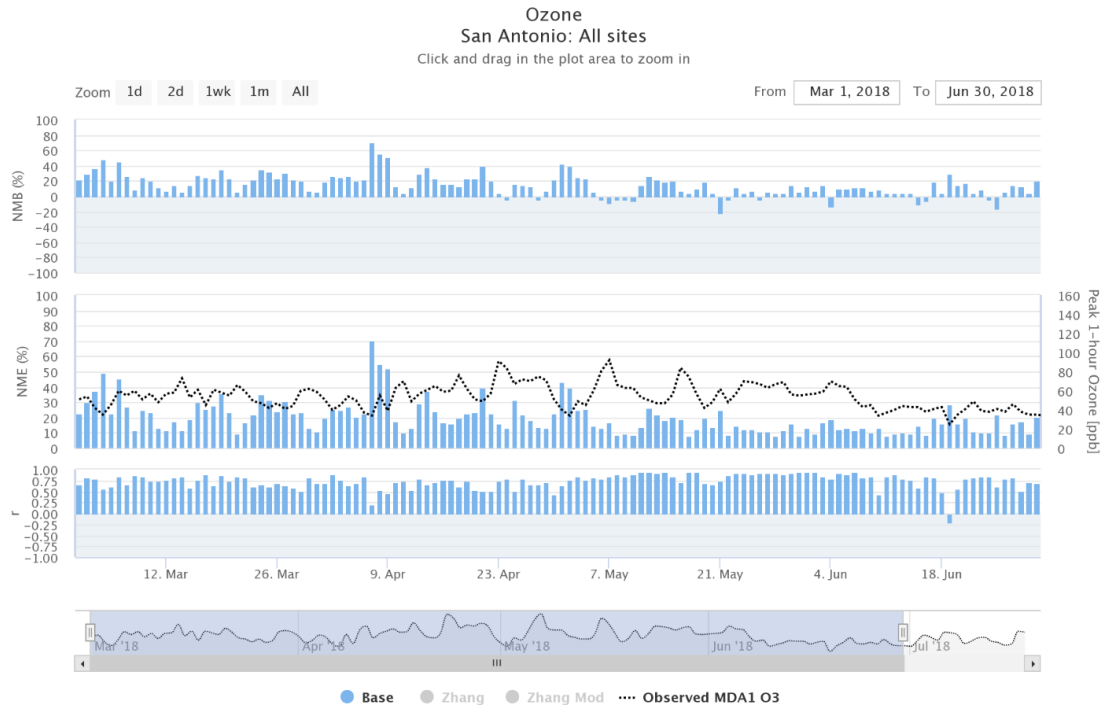

Figure 4-14. San Antonio model performance statistics for ozone (20 ppb cutoff) by area for the base simulation for March 1 – June 30, 2018.

4.3.4 Daily Maximum 8-hour Ozone Statistics

We present soccer plots for MDA8 ozone (Figure 4-15) for all Texas CAMS (top), Dallas monitors (middle) and Houston monitors (bottom). Overall, we observe good performance – the base model NMB is +12.0% and NME is 18.3% across all Texas sites. Bias is degraded in the Zhang runs (Zhang NMB: +14.4%; Zhang Mod NMB: +13.2%). Error is degraded slightly for the Zhang run (NME: 18.5%) but improves slightly with the Zhang Mod run (NME: 17.7%).

The Dallas plot (middle plot in Figure 4-15) shows even better performance than all Texas sites, with NMB of +6.8% and NME of 14.0%. The Zhang runs again shows degradation in bias (Zhang NMB: +8.9%; Zhang Mod NMB: 8.2%) but the Zhang Mod run shows improvement in error (NME: 13.4%). The Houston plot (bottom plot in Figure 4-15) shows worse performance than all Texas and Dallas monitors (base NMB: +20.8%; NME: 24.6%) with small performance improvements from the Zhang Mod run (NMB: +20.4%; NME: 23.3%).

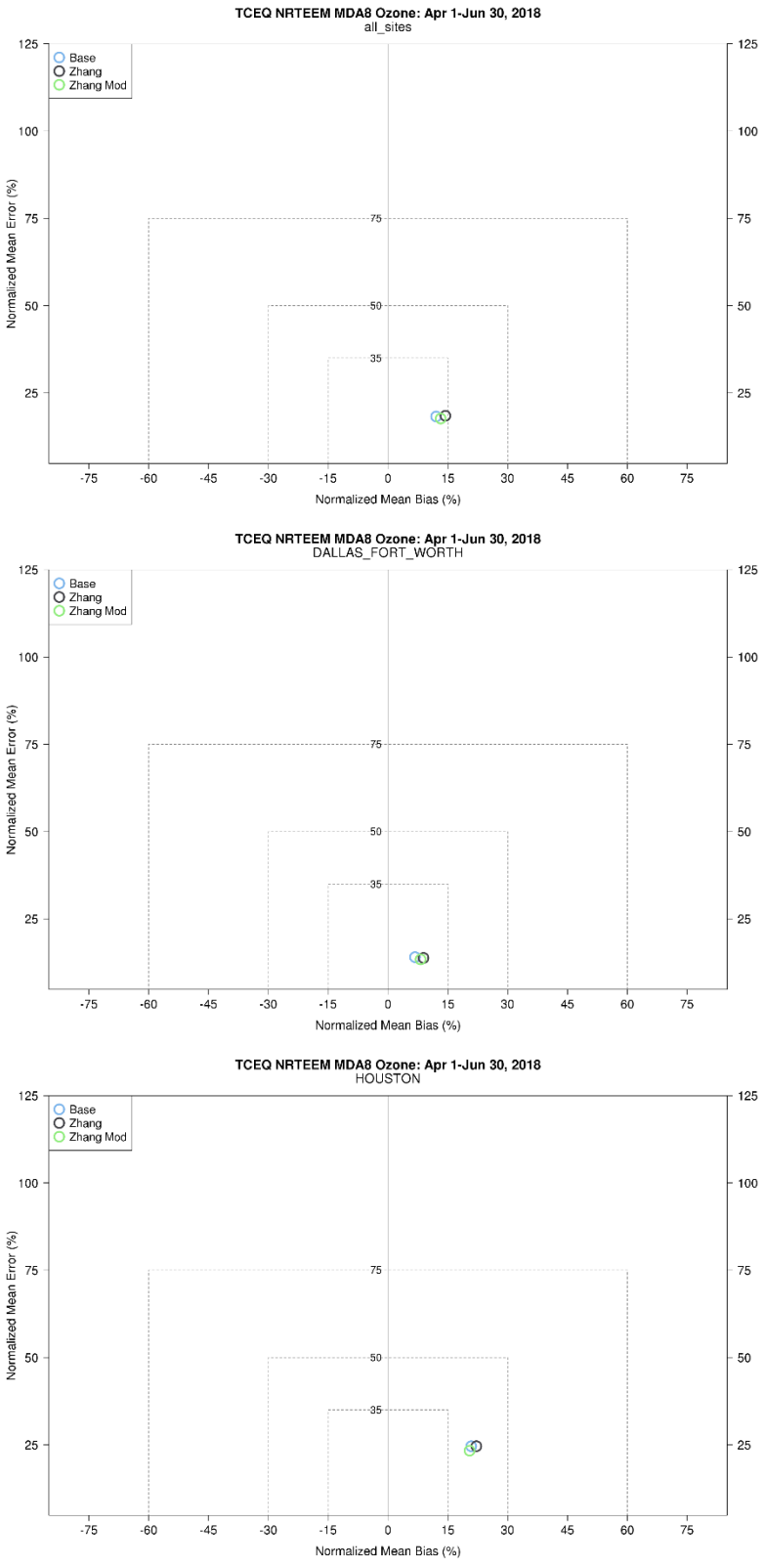

Figure 4-15. Soccer plots for MDA8 ozone for all CAMS in Texas (top), Dallas (middle) and Houston (bottom) covering April 1 - June 30, 2018.

4.3.5 MDA8 Ozone Local Increment

In order to determine how well the base run estimates ozone production in a given metropolitan area, we calculate the MDA8 ozone local increment (LI) for observations and model simulations. The LI of ozone is sensitive to local ozone precursor emissions and the conduciveness of the atmosphere to ozone production on each day. As shown below, the modeled LI of ozone is not very sensitive to choice of dry deposition scheme in CAMx because the LI measures same-day ozone production which allows only a few hours for ozone dry deposition to influence the magnitude of the LI.

Figure 4-16 displays a map of all Dallas-Fort Worth CAMS and a similar map for Houston CAMS is provided in Figure 4-17. We classify the monitors with green pushpins as potential background sites (meaning that when they are upwind of the urban area they are indicative of background) and calculate the median MDA8 ozone concentration across these monitors for each day. Then we find the difference between this background value and the maximum MDA8 ozone concentration across all monitors in the same region. We refer to this difference as the MDA8 ozone LI.

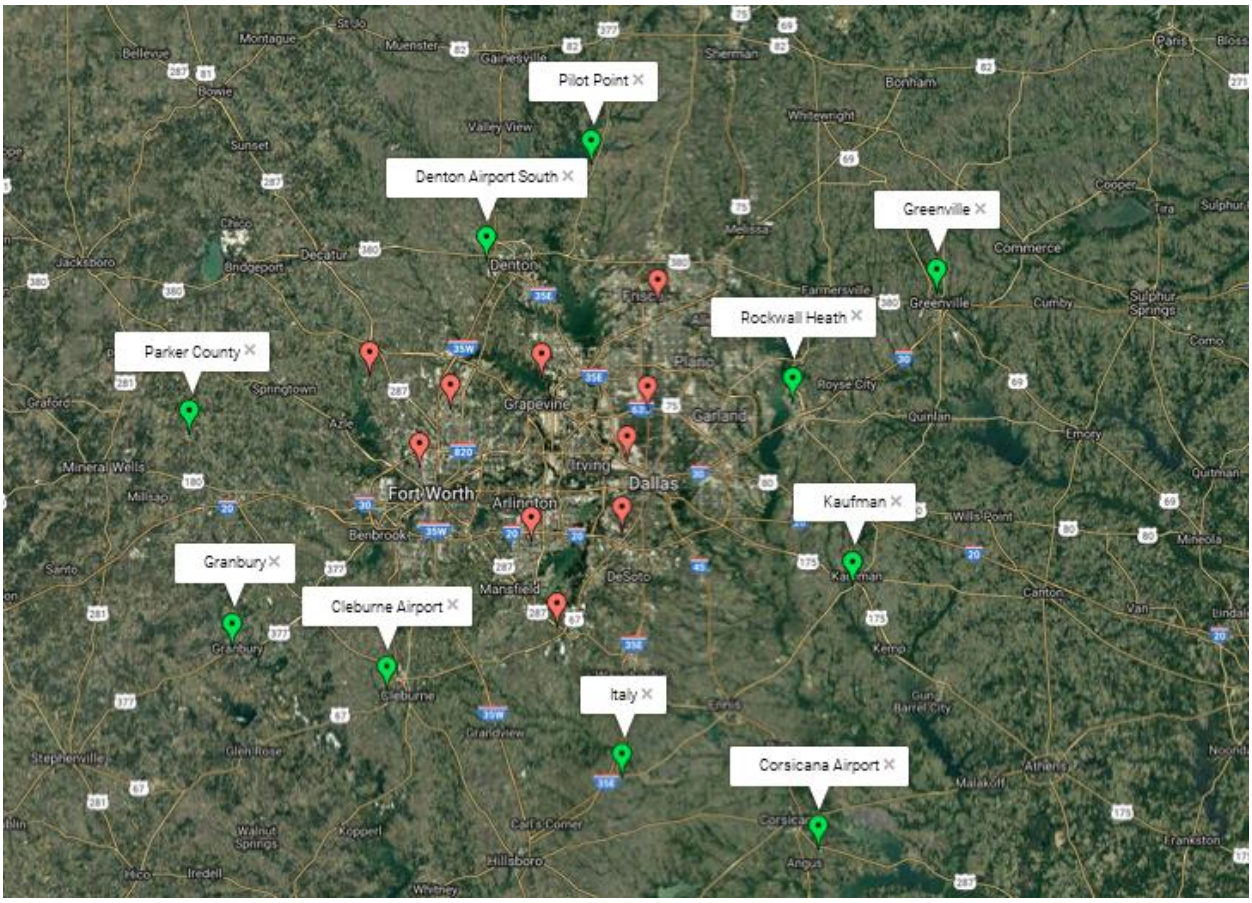

Figure 4-16. Map of Dallas-Fort Worth CAMS monitoring locations. The 10 potential background sites have green markers and are labeled.

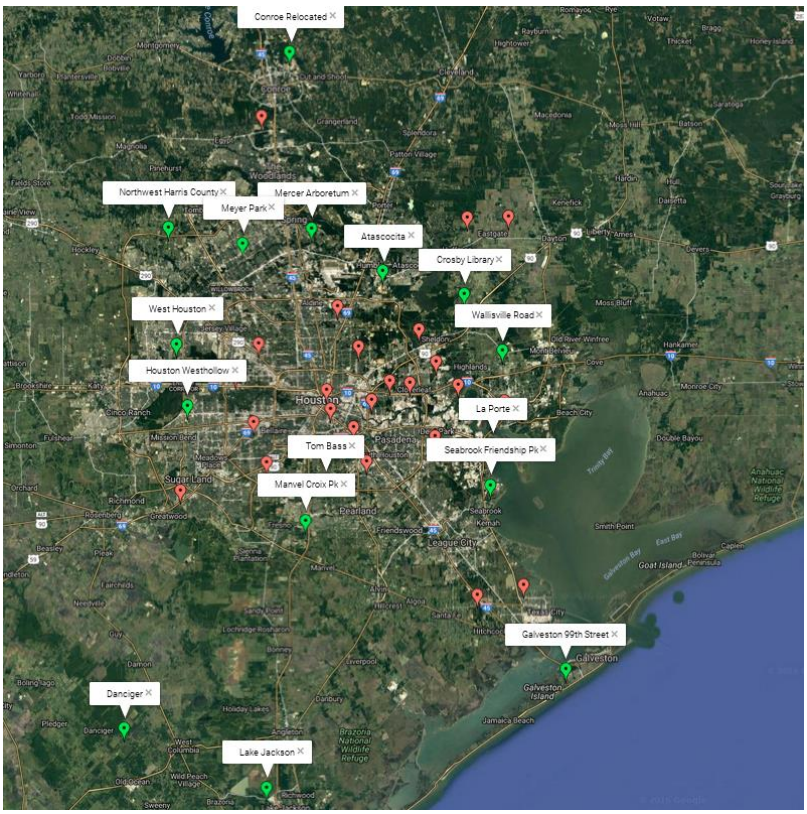

Figure 4-17. Map of Houston CAMS locations. The 16 potential background CAMS have green markers and are labeled.

In Figure 4-18, we present quantile-quantile (Q-Q) plots for Dallas MDA8 ozone local increment for the base model (left panel), Zhang (middle panel) and Zhang Mod (right panel). For each plot, the x-axis shows the observed LI and the y-axis shows each model run's LI. The Dallas plot shows very good agreement for all three models. The plot shows that each model can replicate the full range of observed LI. In contrast to the Dallas plots we see persistent underestimation that occurs throughout the full range of observed LI for Houston (Figure 4-19).

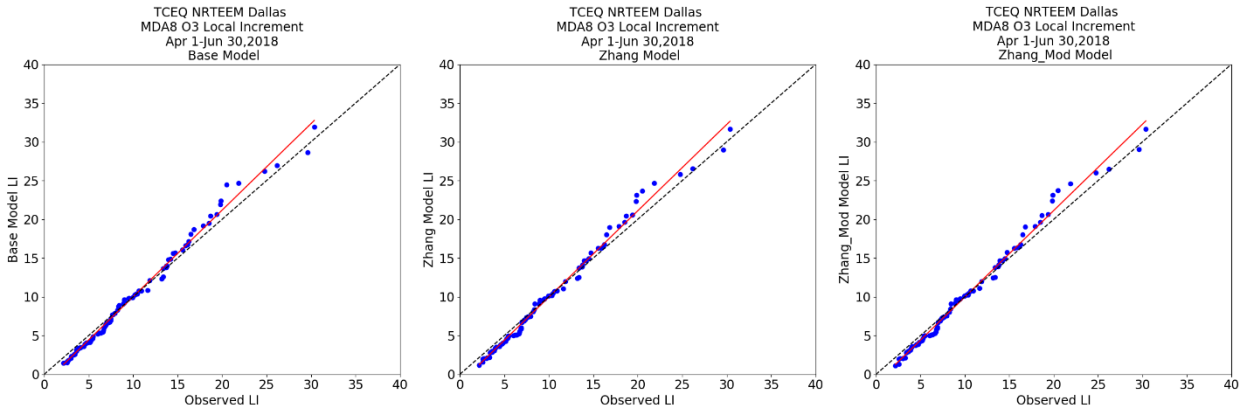

Figure 4-18. Quantile-quantile plots for Dallas MDA8 ozone local increment for the base (left), Zhang (middle) and Zhang Mod (right) simulations.

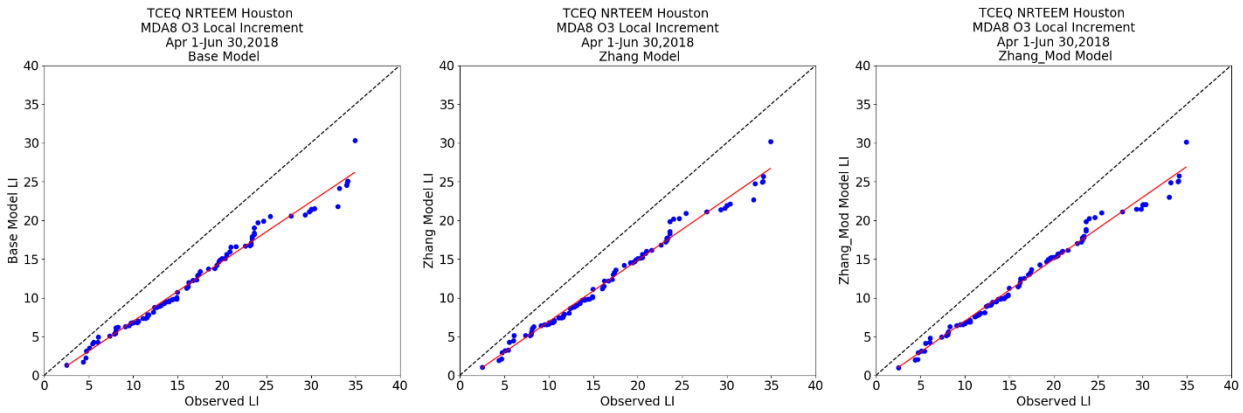

Figure 4-19. Quantile-quantile plots for Houston MDA8 ozone local increment for the base (left), Zhang (middle) and Zhang Mod (right) simulations.

The minor differences found in the MDA8 LI Q-Q plots suggest that the local increment may be relatively insensitive to the changes in ozone deposition we are modeling. To determine the impact of the Zhang simulations on background ozone, we constructed time-paired scatter plots that compare modeled versus observed background MDA8 ozone for each day of the April 1—June 30, 2018 modeling period (Dallas: Figure 4-20; Houston: Figure 4-21). We define background ozone on a given day as the median MDA8 value of all background monitors (green pushpins in Figure 4-16 and Figure 4-17).

Figure 4-20 (Dallas background MDA8 ozone scatter plots) shows that pattern correlation improves substantially for the Zhang simulation (r = 0.804) compared to the base model (r = 0.762). There is a slight improvement in correlation for the Zhang Mod (r = 0.808) compared to the Zhang run. While the base model has the lowest bias (NMB: 5.7%; Zhang: 7.3%; Zhang Mod: 8.1%), the Zhang (NME: 11.7%) and Zhang Mod (NME: 12.2%) runs each have better error statistics than the base model (12.6%). These results suggest that the NRTEEM model is performing well at Dallas background monitors. They also suggest that there may be a slight

positive systematic bias present in the Zhang deposition scheme that if corrected, could result in overall superior performance compared to the base model.

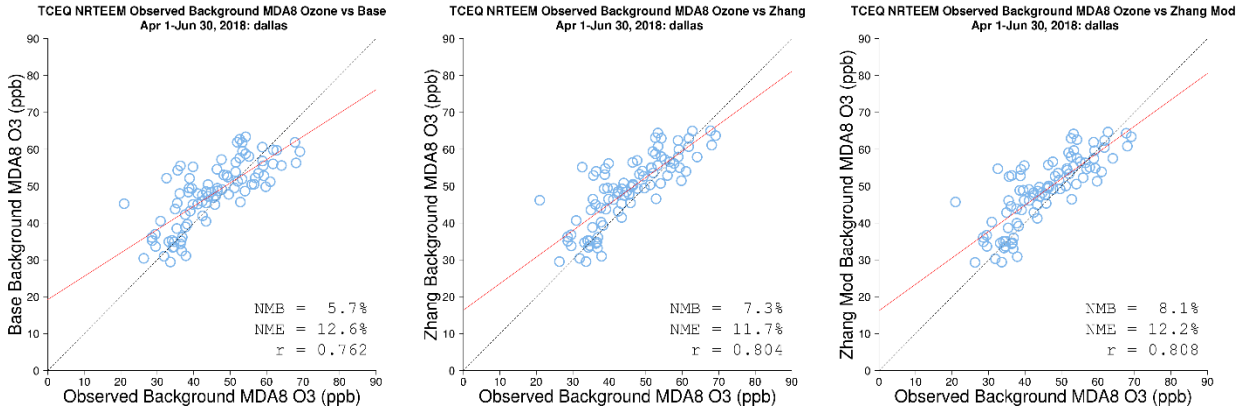

Figure 4-20. Modeled versus observed background MDA8 ozone at Dallas monitors for each day of the Apr 1-Jun 30, 2018 modeling episode for the base model (left), Zhang (middle) and Zhang Mod (right).

Similar to the Dallas plots in Figure 4-20, Figure 4-21 (Houston background MDA8 ozone scatter plots) shows that pattern correlation improves substantially for the Zhang simulation (r = 0.919) compared to the base model (r = 0.888). There is a very slight improvement in correlation for the Zhang Mod (r = 0.920) compared to the Zhang run. The Zhang run has the lowest bias (Zhang NMB: 18.6%; base: 19.0%; Zhang Mod: 20.3%) and the lowest error (Zhang NME: 19.1%; base: 20.5%; Zhang Mod: 20.7%). For each of the three simulations, the NMB is very close to the NME. This suggests that positive biases explain nearly all of the error. This effect is made slightly worse by the Zhang simulations and is evidenced by nearly all of the symbols located to the left side of the 1:1 lines in Figure 4-21. The persistent positive biases at Houston background monitors may be partially related to ozone overestimations over relatively clean Gulf air.

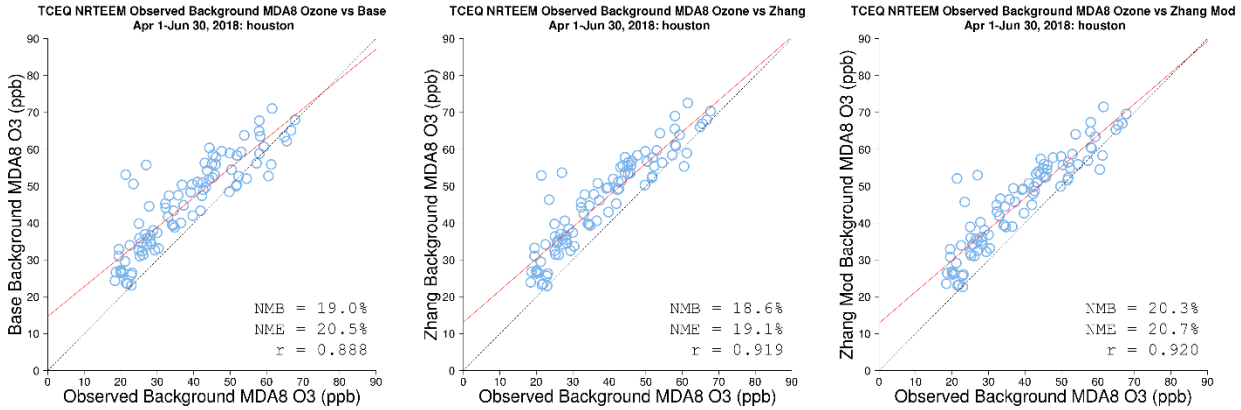

Figure 4-21. Modeled versus observed background MDA8 ozone at Houston monitors for each day of the Apr 1-Jun 30, 2018 modeling episode for the base model (left), Zhang (middle) and Zhang Mod (right).

4.3.6 Exceptional Event Impacts and Model Bias

In this section, we examine the relationship between exceptional event impacts and model bias to determine how model performance is affected by the exceptional events. Figure 4-22 shows density scatter plots of MDA8 ozone bias (x-axis) and modeled fire impacts on MDA8 ozone (y-axis) at CAMS locations in the Dallas-Fort Worth (top left), Houston (top right), San Antonio (bottom left) and El Paso (bottom right) regions for the March – June 2018 period. The vertical dashed lines show the MDA8 ozone mean bias across all CAMS locations in each region for the same period. The plots show that there are relatively few days where the MDA8 ozone impacts from fires exceed 1 ppb. For days when the MDA8 ozone value is greater than 1 ppb, no clear relationship exists between model bias and fire impacts.

Figure 4-23 shows the same set of density scatter plots but for Mexican anthropogenic emissions. As expected, the plots show impacts from Mexican emissions are larger and have much more variation in magnitude in El Paso than the other three regions. The plots suggest no clear impacts from Mexican anthropogenic emissions for any of the four regions. For El Paso, the spread of biases for a given Mexican emissions impact indicates that other factors are likely having a larger influence on model bias.

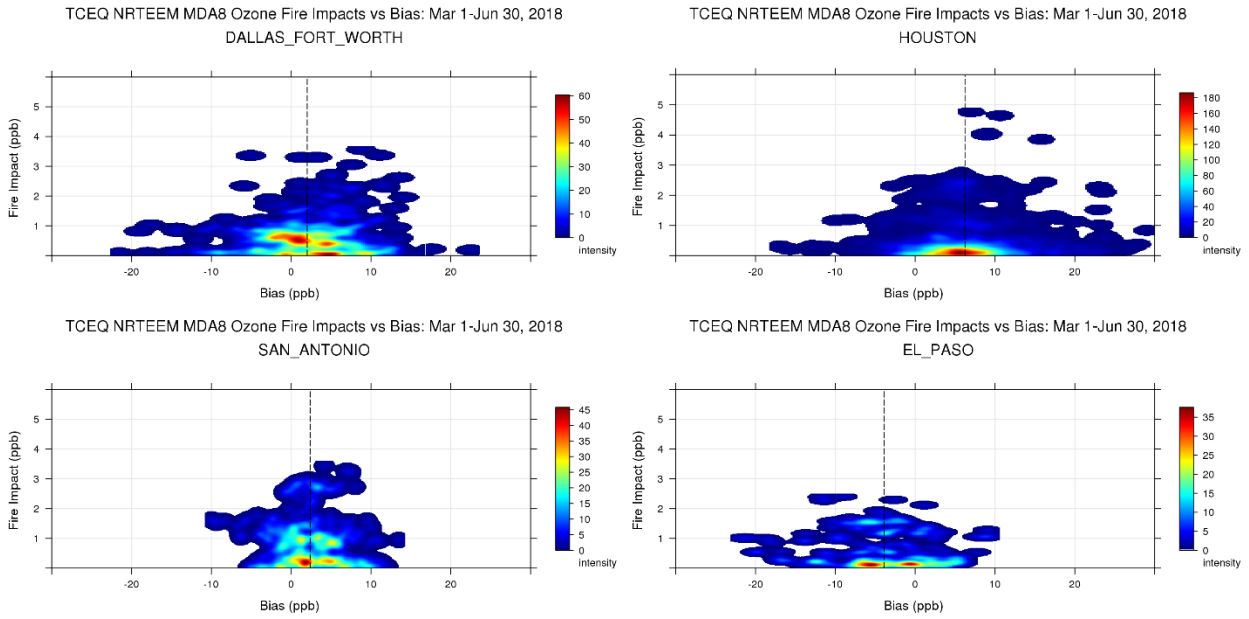

Figure 4-22. Density scatter plots of MDA8 ozone bias and fire impacts at CAMS monitors in the Dallas-Fort Worth (top left), Houston (top right), San Antonio (bottom left) and El Paso (bottom right) regions during March – June 2018. Vertical dashed line represents the mean bias for the base model for the March – June 2018 period.

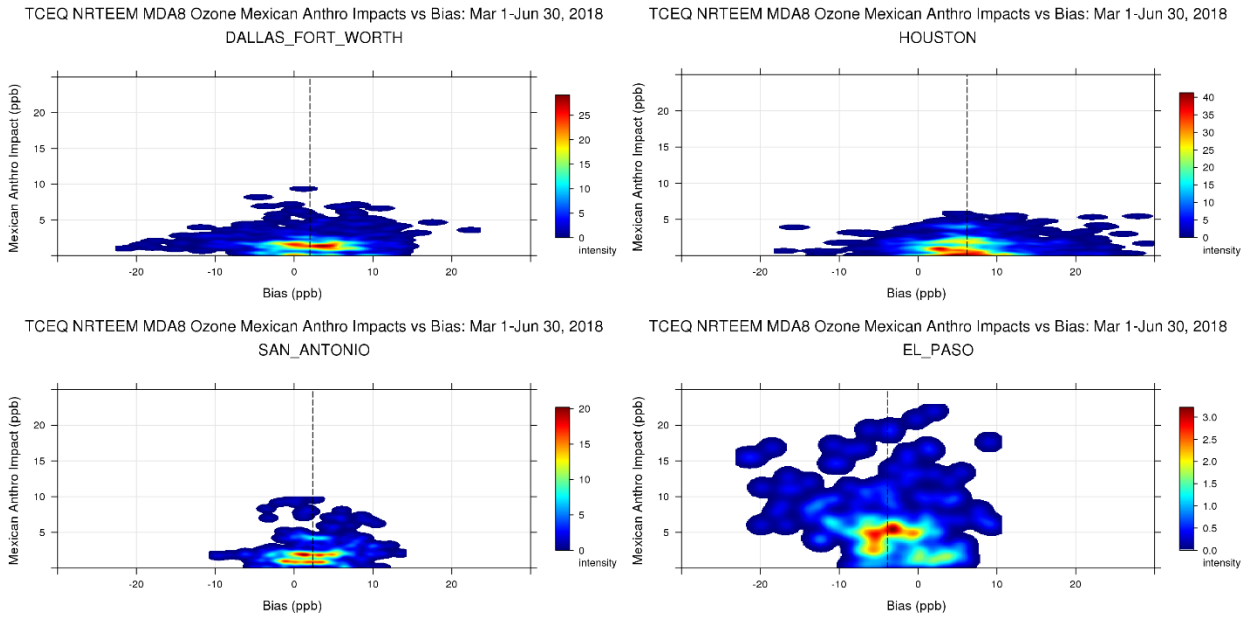

Figure 4-23. Density scatter plots of MDA8 ozone bias and Mexican anthropogenic emissions impacts at CAMS in the Dallas-Fort Worth (top left), Houston (top right), San Antonio (bottom left) and El Paso (bottom right) regions during March – June 2018. Vertical dashed line represents the mean bias for the base model for the March – June 2018 period.

Finally, we present the Stratospheric Ozone impacts in Figure 4-24. These plots suggest very small and infrequent impacts for all regions except El Paso. But again, the plots suggest no clear impacts from stratospheric ozone. The relatively low magnitude of stratospheric ozone is likely underestimated by the NRTEEM system due to only counting ozone impacts from the top of the model and not from the lateral boundaries.

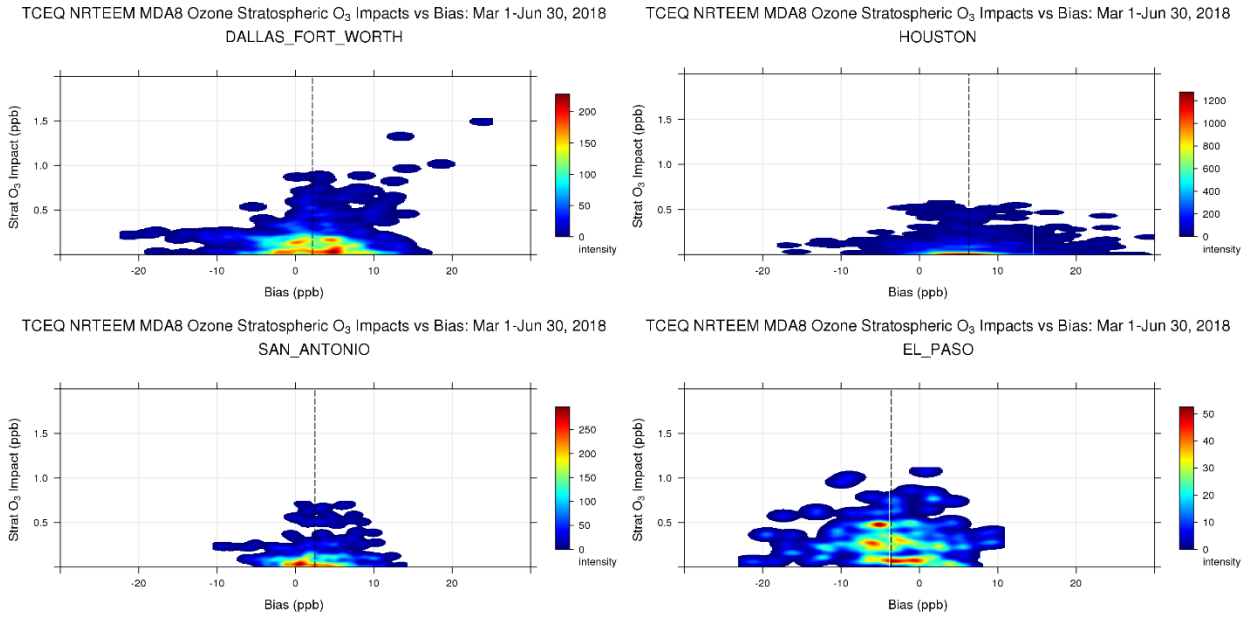

Figure 4-24. Density scatter plots of MDA8 ozone bias and stratospheric ozone impacts at CAMS in the Dallas-Fort Worth (top left), Houston (top right), San Antonio (bottom left) and El Paso (bottom right) regions during March – June 2018. Vertical dashed line represents the mean bias for the Stratospheric Ozone simulation for the March – June 2018 period.

4.4 Potential Exceptional Event Case Studies

In this section, we present evidence for potential exceptional events. This analysis is preliminary. The observed MDA8 values presented in this section are subject to change.

4.4.1 Fire Impacts

As of the time of this writing (July 20, 2018), Camp Bullis (CAMS 58) in San Antonio has a 2016-2018 3-year average of the 4HMDA8 of 71 ppb (see Figure 4-25). The 2018 4HMDA8 is 72 ppb and occurred on April 28, 2018 (see Figure 4-26). The next highest 2018 MDA8 to-date (i.e. 5th highest MDA8 of 2018) is only 66 ppb and occurred the next day, April 29. Camp Bullis (CAMS 58) would need its 2018 4HMDA8 to be 71 ppb or lower to attain EPA's NAAQS for ozone (less than 71 ppb) for 2016-2018. This is a preliminary analysis that does not account for the complete ozone season – Camp Bullis (CAMS 58) recorded 3 of its 4 highest MDA8 ozone values in August-October for each of the 2016 and 2017 years. However, it is important to highlight potential exceptional events so that they can be identified and investigated further if needed.

San Antonio					
Camp Bullis C58	1	69	72	72	**71**
Calaveras Lake C59	1	62	65	66	**64**
San Antonio Northwest C23	2	71	73	67	**70**

Figure 4-25. 2016-2018 4th highest MDA8 ozone values and 3-year average for San Antonio CAMS. Figure from TCEQ website accessed on July 20, 2018.

San Antonio														
San Antonio Northwest C23	2	05/07/2018	1000	**75**	04/23/2018	1200	**73**	04/28/2018	1000	**69**	04/24/2018	1100	**67**
Camp Bullis C58	1	05/07/2018	0900	**83**	04/23/2018	1200	**77**	04/24/2018	0900	**73**	04/28/2018	1000	**72**
Calaveras Lake C59	1	05/07/2018	1100	**71**	05/06/2018	1100	**71**	04/28/2018	1000	**68**	04/24/2018	1100	**66**
Elm Creek Elementary C501	1 N	05/06/2018	1100	**67**	05/07/2018	1000	**66**	04/28/2018	1000	**65**	04/23/2018	1100	**62**
Fair Oaks Ranch C502	1 N	05/07/2018	1100	**79**	04/28/2018	1000	**72**	04/24/2018	1100	**69**	04/23/2018	1300	**67**
Bulverde Elementary C503	1 N	05/07/2018	1100	**78**	04/28/2018	1000	**70**	04/24/2018	1100	**69**	04/23/2018	1200	**68**
New Braunfels Airport C504	1 N	05/07/2018	1000	**67**	04/28/2018	1000	**64**	04/24/2018	1100	**63**	05/06/2018	1000	**61**
City of Garden Ridge C505	1 N	05/07/2018	1000	**75**	05/16/2018	1100	**73**	04/23/2018	1200	**71**	04/28/2018	1000	**68**
Seguin Outdoor Learning Center C506	1 N	04/28/2018	1000	**65**	05/07/2018	1000	**63**	05/06/2018	1100	**63**	04/27/2018	1100	**61**
Heritage Middle School C622	1 N	05/06/2018	1100	**73**	05/07/2018	1200	**68**	04/28/2018	1100	**65**	04/24/2018	1200	**63**
CPS Pecan Valley C678	1 N	05/06/2018	1000	**71**	05/07/2018	1000	**69**	05/16/2018	1100	**60**	05/08/2018	1100	**54**
Government Canyon C1610	1 N	05/07/2018	1000	**67**	04/24/2018	1100	**67**	04/23/2018	1100	**66**	04/28/2018	0900	**65**

Figure 4-26. Dates and MDA8 ozone values for the four highest MDA8 ozone days of 2018 to date as of July 2018 for San Antonio CAMS. Figure from TCEQ website accessed on July 20, 2018.

In Figure 4-27, we present ozone time series (black dotted line: observations; blue line: base model; No Fires: black) for April 28, 2018 at Camp Bullis (CAMS 58). We find that the base model underestimated midday ozone (-8.1 ppb at 12:00 CST) and showed an impact from wildfire emissions of 1.1 ppb. The relatively flat diurnal profile of ozone on this day suggests

that ozone may be of continental origin (which may include ozone produced from wildfire emissions) and not necessarily due to local production.

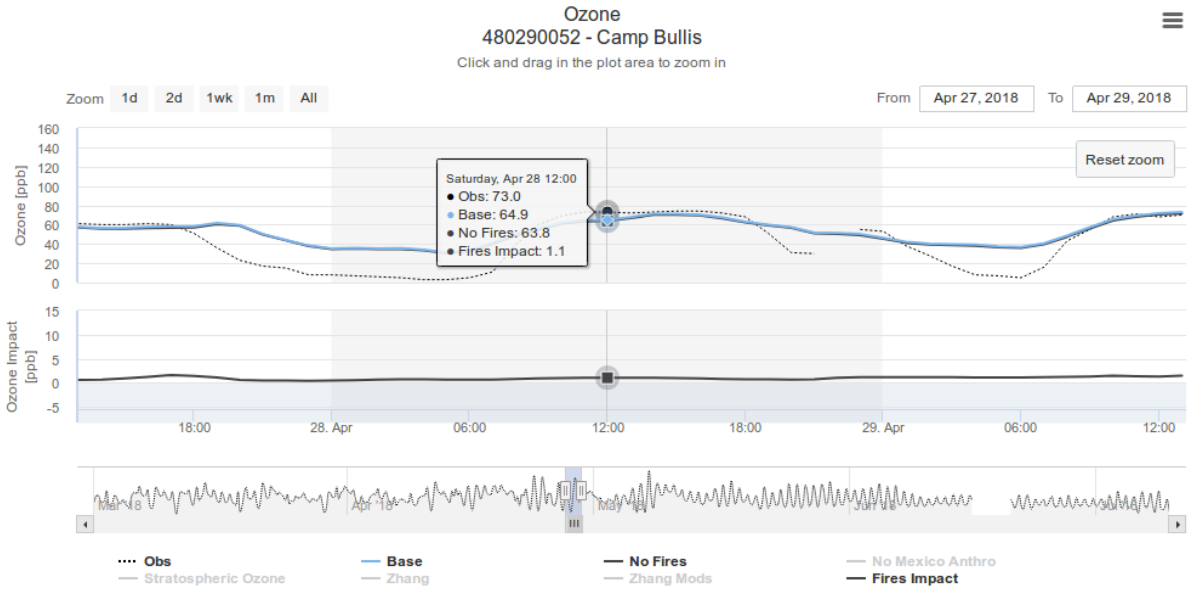

Figure 4-27. Observed (black dotted line), base model (blue) and No Fires sensitivity run differences from base model (black) ozone time series for April 28, 2018 at the Camp Bullis monitor.

National Oceanic and Atmospheric Administration (NOAA)'s Hazard Mapping System (HMS) Analysis Team reported smoke in Oklahoma and eastern Texas on April 28 and traced it to seasonal burning in the Central and South Central U.S.[3]:

[3] http://www.ssd.noaa.gov/PS/FIRE/DATA/SMOKE/2018D281745.html

Saturday, April 28, 2018
DESCRIPTIVE TEXT NARRATIVE FOR SMOKE/DUST OBSERVED IN SATELLITE IMAGERY
THROUGH 1700Z April 28, 2018

SMOKE:
Oklahoma...
Leftover patches of thinner density smoke from a large amount of seasonal fire activity yesterday over the Central and South Central US could be seen over Oklahoma spreading to the southeast.

Central US...
Many new seasonal fires were beginning to be detected in satellite imagery over the Central US from The Dakotas and Minnesota southward to eastern Texas. A number of smoke plumes were also beginning to develop with some of these fires as well.

TCEQ's Daily Air Quality Forecast also mentioned the presence of smoke and its origin in its 4/28 report (emphasis added in bold):

Saturday 04/28/2018
Lingering elevated incoming background levels behind a second departing front when combined with sufficient local add-on could be enough for ozone to reach "Unhealthy for Sensitive Groups" mainly on the northwest side of the Austin, Dallas-Fort Worth, Houston, San Antonio, and Waco-Killeen areas, and the northeast side of the Beaumont-Port Arthur area, and "Moderate" in parts of the Amarillo, Corpus Christi, El Paso, Lubbock, Midland-Odessa, Tyler-Longview, and Victoria areas, with highest concentrations in the afternoon and early evening.

Slightly increased fine particulate background levels associated with building continental haze, **including contributions from residual light smoke should seasonal burning across the South and Southeastern US** continue, could be enough to raise the daily PM2.5 AQI to the lower end of the "Moderate" range primarily in parts of the Beaumont-Port Arthur and Houston areas.

Next, we present the wildfire emissions impact on MDA8 ozone on April 28, 2018 as modeled by the NRTEEM in Figure 4-28. Near the Camp Bullis (CAMS 58) location, MDA8 ozone impacts from wildfires are in the range of 0.8-1.0 ppb.

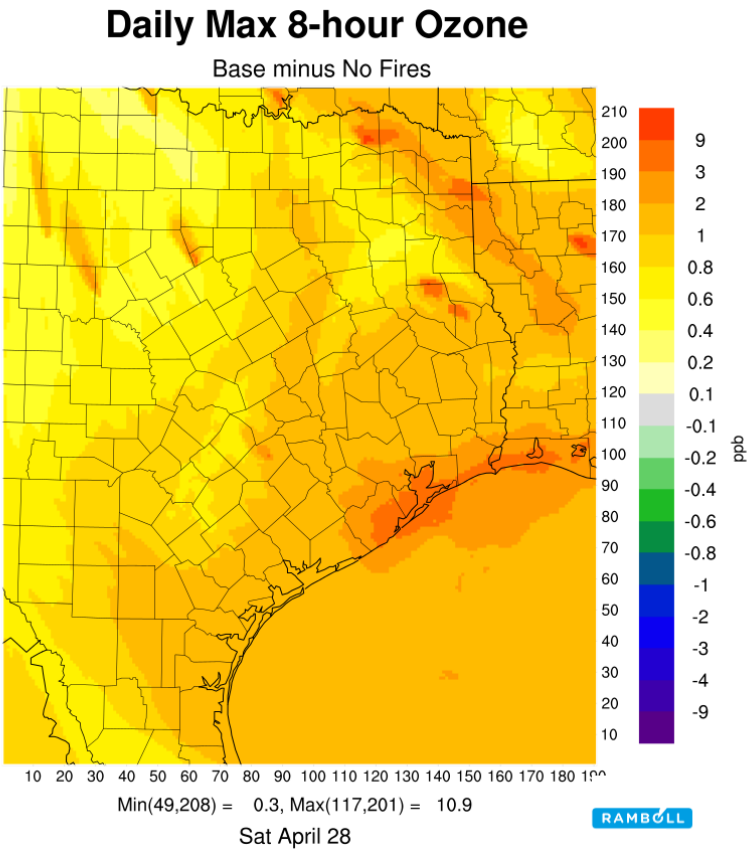

Figure 4-28. MDA8 ozone impacts (ppb) from wildfire emissions (Base-No Fires) for the CAMx 4 km domain on April 28, 2018.

During the period of July 25 – August 4, 2018, Houston, Beaumont-Port Arthur, Dallas, Fort Worth, San Antonio, Waco, Killeen-Temple, Corpus Christi and Tyler ozone monitors all recorded MDA8 values exceeding 70 ppb. Out of 179 exceedances during this period, 67 occurred when NRTEEM fire impacts equalled or exceeded 0.7 ppb (1% of the NAAQS). Table 4-1 lists each of these events. These are potential fire contributions that might or might not be relevant to attainment for an area depending upon whether they are in the top four highest MDA8 observations at the end of the ozone season and whether the monitor ends up determining the attainment status for an area.

Table 4-1. CAMS observed MDA8 ozone (ppb) and NRTEEM Modelled Fire Impacts on MDA8 ozone (ppb) for each day where CAMS observed MDA8 exceeded 70 ppb and fire impacts were equal to or greater than 0.7 ppb for the July 25 – August 4, 2018 period.

Date	Region	Site	Observed MDA8 Ozone (ppb)	Modelled Fire Impact on MDA8 (ppb)
7/25/2018	HOUSTON	UH Moody Tower	71	1.4
7/25/2018	HOUSTON	Houston Croquet	72	1.3
7/25/2018	HOUSTON	Manvel Croix Park	71	1.1

7/25/2018	HOUSTON	Park Place	72	0.9
7/25/2018	AUSTIN	Austin Northwest	74	0.9
7/26/2018	HOUSTON	Houston Deer Park #2	85	1.6
7/26/2018	HOUSTON	Houston Monroe	82	1.6
7/26/2018	HOUSTON	Tom Bass	77	1.5
7/26/2018	HOUSTON	Houston Croquet	84	1.4
7/26/2018	HOUSTON	Conroe Relocated	72	1.3
7/26/2018	SAN ANTONIO	Elm Creek Elementary	71	1.3
7/26/2018	AUSTIN	CAPCOG San Marcos Staples Road	74	1.2
7/26/2018	SAN ANTONIO	Camp Bullis	73	1.2
7/26/2018	DALLAS/FORT WORTH	Greenville	78	1.2
7/26/2018	DALLAS/FORT WORTH	Keller	75	1.2
7/26/2018	HOUSTON	Park Place	79	1.1
7/26/2018	SAN ANTONIO	San Antonio Northwest	72	1.1
7/26/2018	HOUSTON	Manvel Croix Park	92	1.1
7/26/2018	HOUSTON	Texas City 34th Street	81	1.0
7/26/2018	SAN ANTONIO	Government Canyon	71	1.0
7/26/2018	DALLAS/FORT WORTH	Rockwall Heath	79	1.0
7/26/2018	DALLAS/FORT WORTH	Frisco	84	1.0
7/26/2018	HOUSTON	Houston Aldine	75	0.9
7/26/2018	DALLAS/FORT WORTH	Pilot Point	72	0.9
7/26/2018	HOUSTON	UH Moody Tower	83	0.9
7/26/2018	HOUSTON	Seabrook Friendship Park	82	0.9
7/26/2018	DALLAS/FORT WORTH	Dallas North #2	90	0.9
7/26/2018	HOUSTON	Houston Bayland Park	77	0.9
7/26/2018	DALLAS/FORT WORTH	Grapevine Fairway	82	0.9
7/26/2018	HOUSTON	Lang	74	0.9
7/26/2018	DALLAS/FORT WORTH	Dallas Hinton	81	0.9
7/26/2018	AUSTIN	Austin Northwest	71	0.9
7/26/2018	DALLAS/FORT WORTH	Denton Airport South	71	0.9
7/26/2018	HOUSTON	Galveston 99th Street	107	0.7
7/27/2018	HOUSTON	Channelview	87	1.8
7/27/2018	HOUSTON	Houston East	94	1.5
7/27/2018	HOUSTON	HRM #3 Haden Rd	91	1.4
7/27/2018	HOUSTON	Houston North Wayside	90	1.3
7/27/2018	HOUSTON	Wallisville Road	81	1.2
7/27/2018	HOUSTON	Baytown Garth	81	1.2
7/27/2018	DALLAS/FORT WORTH	Greenville	87	1.1
7/27/2018	AUSTIN	Austin Northwest	71	0.8
7/27/2018	HOUSTON	Lynchburg Ferry	86	0.8
7/27/2018	DALLAS/FORT WORTH	Keller	73	0.8

7/27/2018	HOUSTON	Lang	100	0.7
7/28/2018	HOUSTON	Crosby Library	82	1.6
7/28/2018	DALLAS/FORT WORTH	Grapevine Fairway	75	1.3
7/28/2018	HOUSTON	Wallisville Road	71	1.3
7/28/2018	HOUSTON	Baytown Garth	71	1.3
7/28/2018	DALLAS/FORT WORTH	Keller	71	1.2
7/28/2018	DALLAS/FORT WORTH	Frisco	85	1.1
7/28/2018	HOUSTON	Atascocita	85	1.1
7/28/2018	DALLAS/FORT WORTH	Dallas North #2	76	1.0
7/28/2018	TYLER	Tyler Airport Relocated	74	0.9
7/28/2018	HOUSTON	UH WG Jones Forest	85	0.8
7/29/2018	EL PASO	Skyline Park	79	0.8
7/29/2018	EL PASO	El Paso UTEP	91	0.8
7/29/2018	EL PASO	El Paso Chamizal	86	0.8
7/29/2018	EL PASO	Ascarate Park SE	75	0.7
7/30/2018	DALLAS/FORT WORTH	Keller	72	0.8
7/31/2018	AUSTIN	CAPCOG San Marcos Staples Road	76	0.7
8/1/2018	HOUSTON	Lake Jackson	77	1.4
8/1/2018	HOUSTON	Seabrook Friendship Park	76	0.9
8/1/2018	HOUSTON	Oyster Creek	94	0.8
8/1/2018	HOUSTON	Texas City 34th Street	96	0.7
8/2/2018	DALLAS/FORT WORTH	Pilot Point	76	0.7
8/3/2018	EL PASO	Ivanhoe	71	1.7

4.4.2 Stratospheric Ozone Impacts

In this section, we present stratospheric ozone impacts. The NRTEEM system is likely underestimating stratospheric ozone impacts because we are only measuring ozone coming through top of the model. There also could be substantial amounts of stratospheric ozone coming through lateral boundaries near the top of the model because the tropopause can be lower than the CAMx top, depending upon location and season.

4.4.2.1 El Paso

We present the ozone time series (observed: black dotted line, base model: blue and stratospheric ozone impacts: red) at El Paso UTEP (CAMS 12) for March 1 – June 30, 2018 in Figure 4-29. There are several times where stratospheric ozone impacts exceed 1 ppb from March through May. However, none of these events occur when observed ozone is high. The largest stratospheric ozone impact in the NRTEEM system happens on April 1 and is 5 ppb. The base model substantially overestimates peak 1-hour ozone on this day (base model: 95.9 ppb; observed: 53.0 ppb). The fact that the base model ozone is so high (where ozone from the top boundary is capped at 100 ppb) suggests that stratospheric ozone may be transported from the lateral boundaries.

Figure 4-30 shows two maps for the 12 km CAMx domain on April 1, 2018: on the left is a map of the MDA8 ozone and on the right is a map of the MDA8 ozone impacts from stratospheric ozone. The two maps show similar spatial patterns in New Mexico, West Texas and Mexico. This finding provides more evidence that ozone of stratospheric origin is coming through high altitude lateral boundaries rather than just the top of the model. For 2019 NRTEEM we will count the influx of stratospheric ozone from the lateral boundaries above the tropopause height in addition to the top boundary. We will also investigate whether 100 ppb is an appropriate value to use for identifying ozone of stratospheric origin.

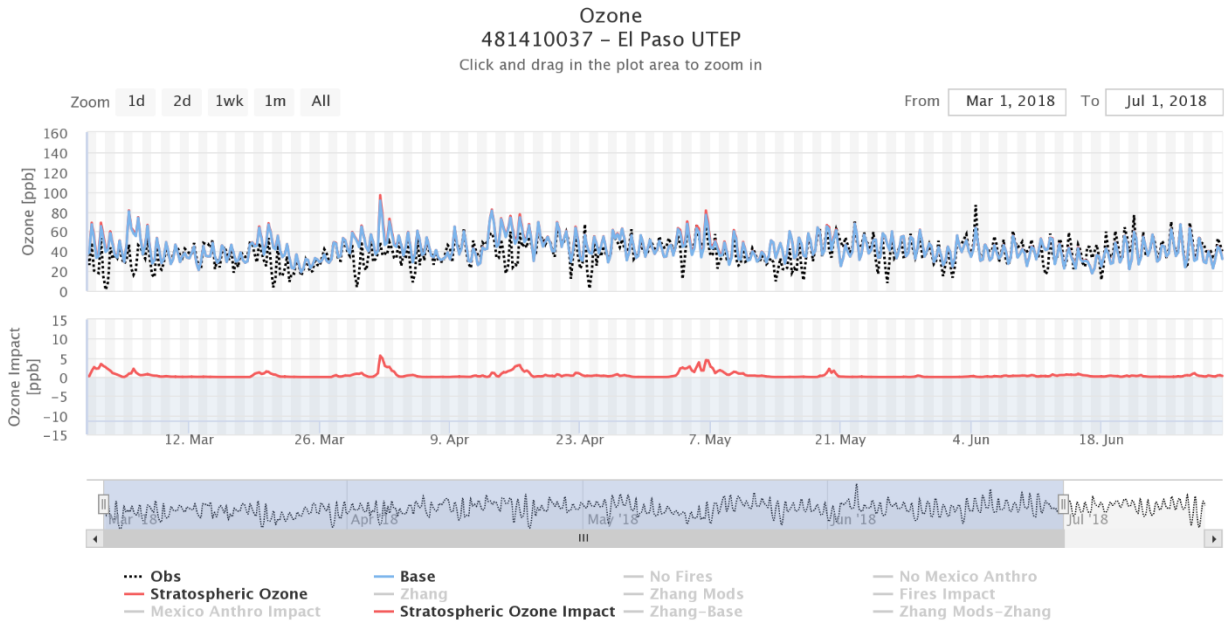

Figure 4-29. Observed (black dotted line), base model (blue), Stratospheric Ozone sensitivity run differences from base model (red) ozone time series for March 1 – June 30, 2018 at El Paso UTEP (CAMS 12) monitor.

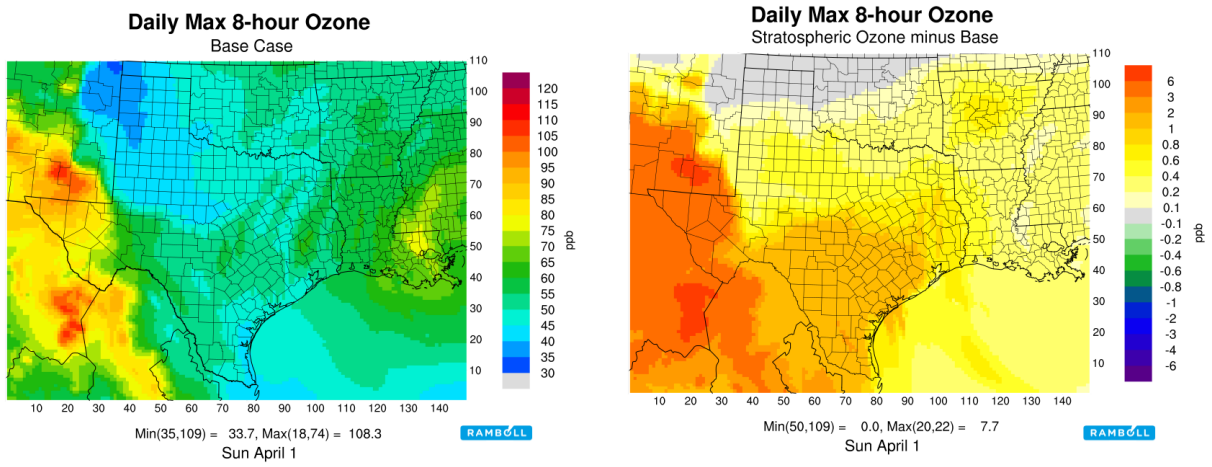

Figure 4-30. MDA8 ozone (ppb; left) and MDA8 ozone impacts from Stratospheric Ozone (Stratospheric Ozone-Base; right) for the CAMx 12 km domain on April 1, 2018.

4.4.2.2 Gothic, Colorado

Previous studies have examined ozone observations at high-elevation EPA Clean Air Status and Trends Network (CASTNET) monitors in the Rocky Mountains to determine impacts of stratospheric ozone at the surface and to investigate vertical ozone transport in models (Stoeckenius et al., 2009; Emery et al., 2011). We added one of these high elevation CASTNET monitors (Gothic, CO; elevation: 2926 m) to the NRTEEM website's time series and statistics pages to track potential stratospheric ozone intrusions. We present ozone time series

(observed: black dotted line; base model: blue; stratospheric ozone impacts: red) at the Gothic monitor for March 1 – June 30, 2018 in Figure 4-31. The time series shows periodic large positive biases. Because these perturbations are occurring in March and April in a remote high elevation location, they are most likely due to stratospheric ozone. The Gothic monitor is located within a 36 km grid cell and we cannot expect the model to perform well with such coarse resolution in complex terrain.

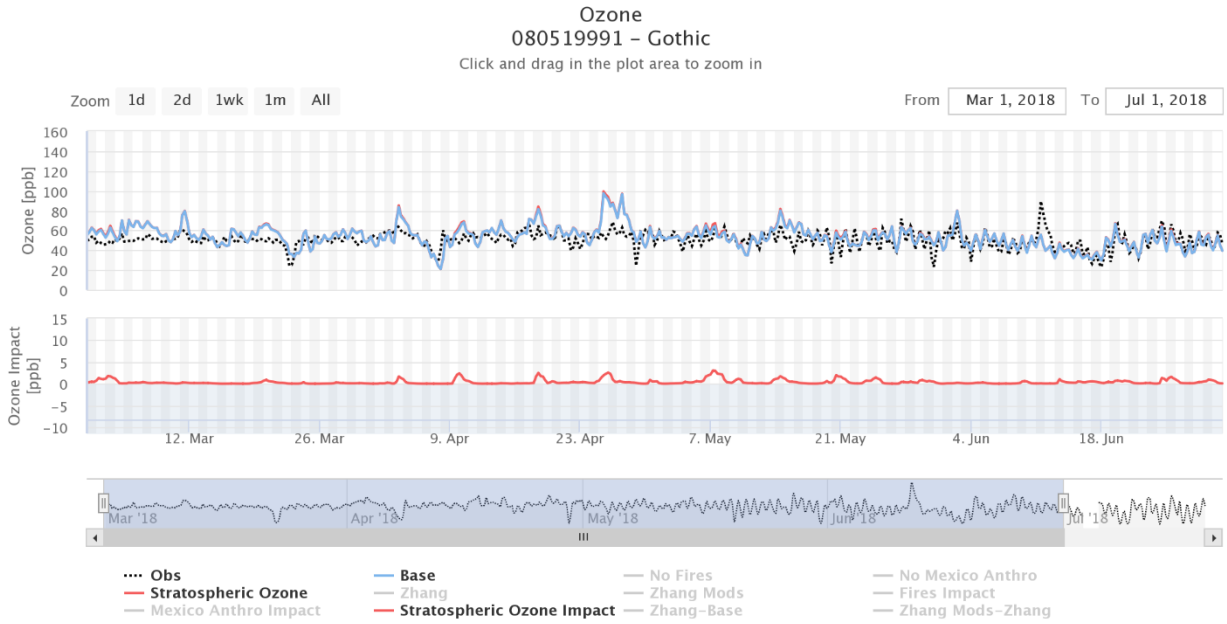

Figure 4-31. Observed (black dotted line), base model (blue), Stratospheric Ozone sensitivity run differences from base model (red) ozone time series for March 1 – June 30, 2018 at the Gothic, CO CASTNET monitor.

4.4.3 Impacts from Mexican Anthropogenic Emissions

Next we examine potential exceptional event impacts from Mexican anthropogenic emissions. The largest ozone impacts in Texas from Mexican anthropogenic emissions tend to occur under a southerly wind regime, when ozone is typically low to moderate (Johnson et al., 2017). There is considerable uncertainty in the Mexico emissions inventory (Shah et al., 2018). While some emissions sources/sectors could be biased high, the inventory could also be missing significant sources.

4.4.3.1 Camp Bullis: April 24, 2018

Camp Bullis (CAMS 58) recorded an MDA8 value of 73 ppb on April 24, 2018. At the time of this writing, this was the 3rd highest MDA8 value (73 ppb) of 2018. The NRTEEM model predicts that Mexico anthropogenic emissions are contributing over 2 ppb in the midday hours at this monitor. Figure 4-32 shows the hourly ozone time series for April 24 and shows the Mexican anthropogenic impact (2.7 ppb) at the time of maximum impact (2:00 PM CST). Wildfire emissions show a smaller impact at this time of day (0.9 ppb), but increase in the late afternoon

(maximum impact is 2.1 ppb at 6:00 PM CST). Figure 4-33 shows a map of the MDA8 ozone impacts from Mexican anthropogenic emissions on April 24. Impacts near Camp Bullis (CAMS 58) are between 0.5 and 1.0 ppb. Areas of map exceeding 1.0 ppb lie just to the northwest of the monitor.

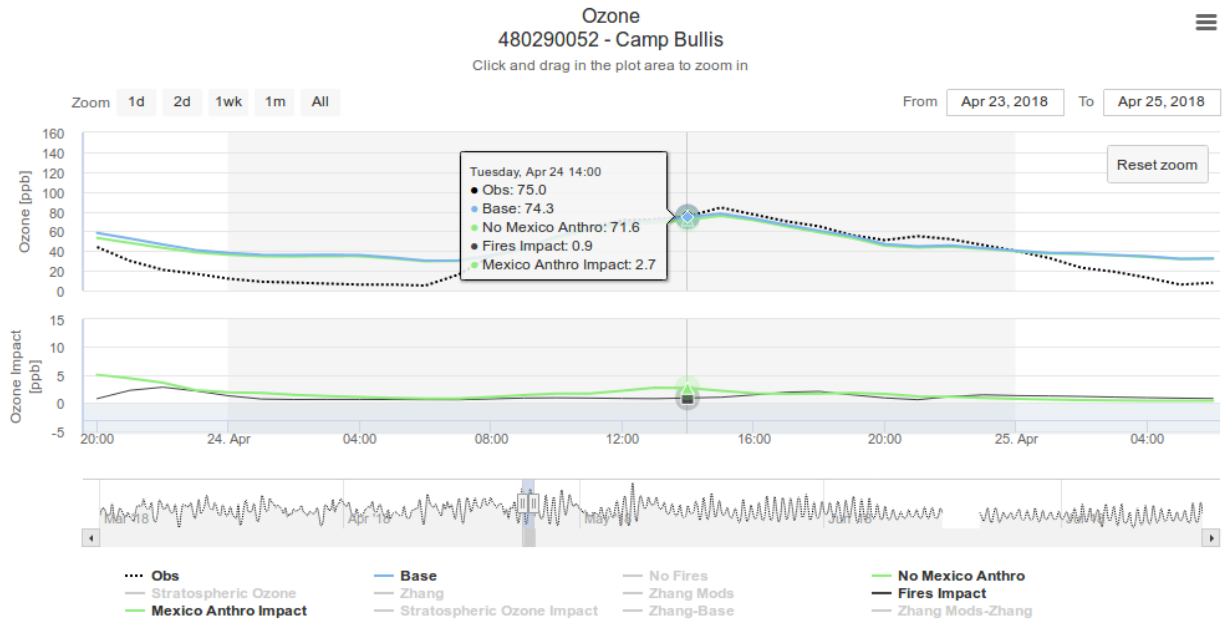

Figure 4-32. Observed (black dotted line), base model (blue), No Mexico Anthro sensitivity run differences from base model (green) ozone time series for April 28, 2018 at Camp Bullis (CAMS 58). Wildfire impacts are shown in black.

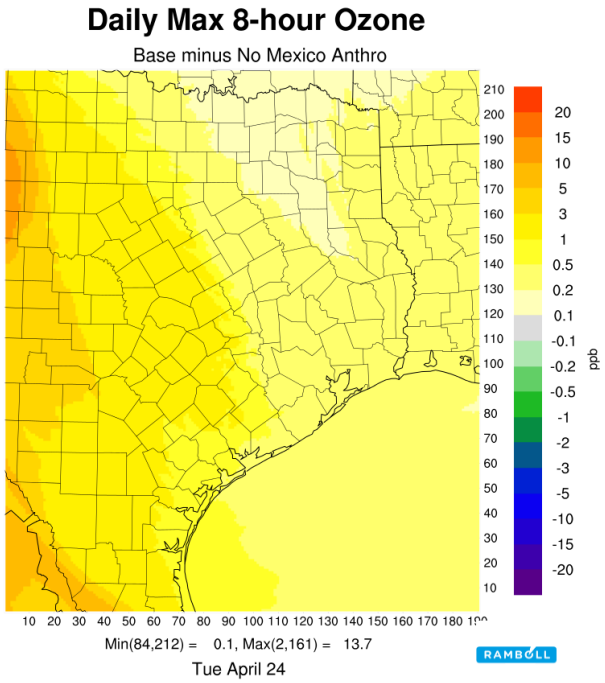

Figure 4-33. MDA8 ozone impacts (ppb) from Mexican anthropogenic emissions (Base-No Mexico Anthro) for the CAMx 4 km domain on April 24, 2018.

4.4.3.2 El Paso UTEP: May 22, 2018

As of the time of this writing (July 20, 2018), the El Paso UTEP (CAMS 12) monitor has a 2016-2018 3-year average of the 4HMDA8 of 71 ppb (see Figure 4-34). The 2018 4HMDA8 is 68 ppb and occurred on May 22, 2018 (see Figure 4-35). The next highest 2018 MDA8 to-date (i.e. 5th highest MDA8 of 2018) is only 66 ppb and occurred on June 26. El Paso UTEP (CAMS 12) would need its 2018 4HMDA8 to be 67 ppb or lower to attain EPA's NAAQS for ozone (less than 71 ppb) for 2016-2018. As mentioned in Section 4.5.1, this is a preliminary analysis that does not account for the complete ozone season.

El Paso-Juarez					
Ivanhoe C414	1	59	63	65	**62**
El Paso UTEP C12/A125/X151	2	71	74	68	**71**
Socorro Hueco C49/F312	1	64	62	61	**62**
Skyline Park C72	1	66	75	72	**71**
Chamizal C41/AH126	1	65	72	68	**68**
Ascarate Park SE C37/A332/A172/X159	1	66	67	65	**66**

Figure 4-34. 2016-2018 3-year averages of the 4th highest MDA8 ozone for El Paso CAMS. Figure from TCEQ website.

El Paso-Juarez														
El Paso UTEP C12/A125/X151	2	06/04/2018	1100	82	06/21/2018	1000	72	06/25/2018	1100	69	05/22/2018	1000	68
Ascarate Park SE C37/A332/A172/X159	1	06/04/2018	1100	82	06/21/2018	1100	70	06/26/2018	1000	65	05/22/2018	1000	65
Chamizal C41/AH126	1	06/04/2018	1100	83	06/21/2018	1100	73	05/22/2018	1000	70	05/19/2018	1100	68
Socorro Hueco C49/F312	1	06/04/2018	1200	70	05/19/2018	1000	62	05/09/2018	1100	62	05/22/2018	1000	61
Skyline Park C72	1	06/04/2018	1100	77	06/21/2018	1100	76	06/27/2018	1000	75	06/26/2018	1000	72
BRAVO Big Bend C67/C316/C656/C691	3 N	04/21/2018	1200	69	05/19/2018	1000	65	05/01/2018	1100	65	04/17/2018	1500	63
Ivanhoe C414	1	06/04/2018	1100	74	05/22/2018	1000	66	05/18/2018	1400	66	05/19/2018	1000	65

Figure 4-35. Dates and MDA8 ozone values for the 4 highest MDA8 ozone days of 2018 to date as of July 2018 for El Paso. Figure from TCEQ website.

The NRTEEM model estimated that Mexico anthropogenic emissions contribute 10.3 ppb to the MDA8 value at this monitor on May 22, 2018. Figure 4-36 shows the hourly ozone time series for the UTEP (CAMS 12) monitor. The maximum hourly Mexican anthropogenic impact is over 17.2 ppb at 2:00 PM CST.

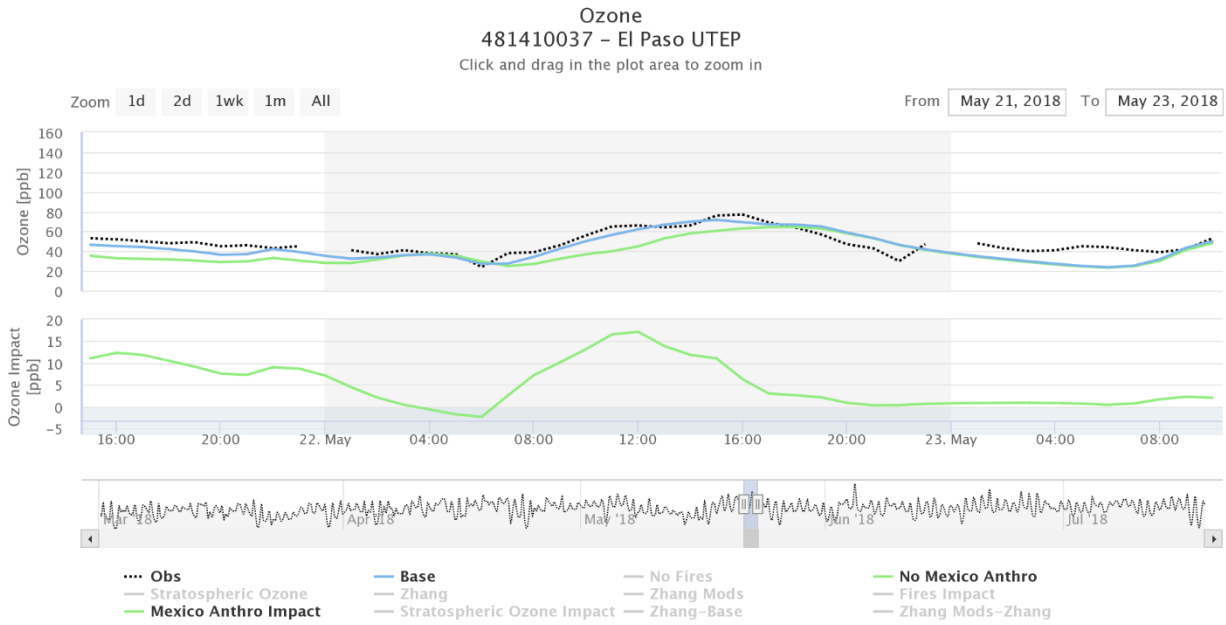

Figure 4-36. Observed (black dotted line), base model (blue), No Mexico Anthro sensitivity run differences from base model (green) ozone time series for May 22, 2018 at El Paso UTEP (CAMS 12).

4.5 Overall Assessment

4.5.1 Main Findings

We performed quantitative and qualitative evaluations of WRF meteorological and CAMx ozone performance. Evaluation of WRF meteorological statistical metrics revealed that the NRTEEM system agreed as well or better with observations than the 2017 FIM system. The objective of the CAMx ozone model performance evaluation was to determine whether the alterative dry deposition schemes (Zhang and Zhang Mod) substantially impact or improve ozone performance.

In general, the Zhang simulation results in higher ozone concentrations (due to lower ozone deposition) compared to the base model. Therefore, when the base model underestimates ozone, the Zhang simulation tends to improve performance. The Zhang Mod simulation results in lower ozone concentrations compared to Zhang, which results in performance similar to the base model.

Next, we examined the local increment (LI) to MDA8 ozone as a way to measure the model's ability to estimate ozone production from emissions in a given metropolitan area. Overall, we found very little difference between the base and Zhang runs. Performance was found to be quite good in Dallas. Consistent with the previous FIM study (Johnson et al., 2017), we found persistent LI underestimates in Houston for both the base and Zhang runs. We evaluated background MDA8 ozone performance in Dallas and Houston and that while the Zhang runs improved correlation, bias and error performance was mixed.

Finally, we examined relationships between modeled exceptional event impacts and base case model bias. If such relationships existed they might indicate that the modeled exceptional event impacts were themselves biased. We find no clear relationship between any of the exceptional event impacts and NRTEEM base case model bias.

4.5.2 Exceptional Event Impact Summary

NRTEEM includes three sensitivity simulations to identify potential exceptional events. The first quantifies ozone impacts from biomass burning and found a potential exceptional event at Camp Bullis (CAMS 58) in San Antonio on April 28, 2018. During the high ozone period of July 25 – August 4, 2018, we found 67 occurrences where observed MDA8 ozone exceeded 70 ppb and NRTEEM fire impacts equalled or exceeded 0.7 ppb (1% of the NAAQS). These are potential fire contributions that might or might not be relevant to attainment for an area depending upon whether they are in the top four highest MDA8 observations at the end of the ozone season and whether the monitor ends up determining the attainment status for an area. The second simulation examines stratospheric ozone intrusions. While we find some stratospheric ozone impacts in El Paso, the impacts did not occur when observed ozone was high so we did not find any potential exceptional events. The third simulation quantifies ozone impacts of Mexico anthropogenic emissions, which may not fit within the regulatory definition of an exceptional event, and we found two potential exceptional events at San Antonio and El Paso monitors.

The NRTEEM system implements and refines the photochemical grid model system used by the TCEQ for State Implementation Plan (SIP) modeling by modeling exceptional event impacts in a NRT mode. The system demonstrates usefulness by identifying potential days when exceptional events may be responsible for ozone exceedances.

5.0 RECOMMENDATIONS FOR IMPROVEMENTS TO MODELING SYSTEM IN 2019

In this section, we make recommendations for a combination of CAMx modeling improvements as well as website improvements for the 2019 modeling system.

5.1 CAMx Modeling Improvements for 2019

We provide the following recommendations to improve the usefulness of the modeling system by including:

- Using the latest available versions of WRF and CAMx model code
- Using new emissions inventory from TCEQ if available
- Working with TCEQ to refine the Mexico emission inventory
- Improving treatment of stratospheric influence by counting influx through lateral boundaries above tropopause height (in addition to influx through top boundary) and adding more vertical layers near the tropopause
- Continuing to investigate sensitivity tests around the base case such as alternate sources of boundary condition
- Performing additional LI analyses for different regions including San Antonio with input from TCEQ

5.2 Website Improvements for 2019

We provide the following recommendations to improve the NRTEEM website by including:

- Using a dedicated machine for hosting NRTEEM website
- Other improvements proposed by TCEQ

6.0 REFERENCES

Emery, C., E. Tai, G. Yarwood, and R. Morris, 2011. Investigation into approaches to reduce excessive vertical transport over complex terrain in a regional photochemical grid model. Atmospheric Environment. 45. 7341-7351. 10.1016/j.atmosenv.2011.07.052.

Ek, M., Bill Lapenta, Geoff DiMego, Hendrik Tolman, John Derber, Yuejian Zhu, Vijay Tallapragada, Mark Iredell, Shrinivas Moorthi, Suru Saha. 2014. The NOAA Operational Numerical Guidance System. 29th Session of the World Weather/Climate Research Programme (WWRP/WCRP) Working Group on Numerical Experimentation (WGNE-29) Bureau of Meteorology, Melbourne, Australia, 10-14 March 2014.

Emery, C., E. Tai, and G. Yarwood, 2001. "Enhanced Meteorological Modeling and Performance Evaluation for Two Texas Ozone Episodes." Prepared for the Texas Natural Resource Conservation Commission, prepared by ENVIRON.

ENVIRON and Alpine. 2012. Western Regional Air Partnership (WRAP) West-wide Jump-start Air Quality Modeling Study (WestJumpAQMS) – WRF Application/Evaluation. ENVIRON International Corporation, Novato, California. Alpine Geophysics, LLC. University of North Carolina. February 29. (http://www.wrapair2.org/pdf/WestJumpAQMS_2008_Annual_WRF_Final_Report_February29_2012.pdf).

Guenther, A., Karl, T., Harley, P.,Wiedinmyer, C., Palmer, Geron, C. 2006. Estimates of global terrestrial isoprene emissions using MEGAN (Model of Emissions of Gases and Aerosols from Nature), Atmos. Chem Phys., 6, 3181-3210.

Johnson, J., E. Tai, P. Karamchandani, G. Wilson, and G. Yarwood. 2013. TCEQ Ozone Forecasting System. Prepared for Mark Estes, TCEQ. November.

Johnson, J., G. Wilson, D.J. Rasmussen, G. Yarwood. 2015. "Daily Near Real-Time Ozone Modeling for Texas." Prepared for Texas Commission on Environmental Quality, Austin, TX. January.

Johnson, J., G. Wilson, D.J. Rasmussen, G. Yarwood. 2016a. "Daily Near Real-Time Ozone Modeling for Texas." Prepared for Texas Commission on Environmental Quality, Austin, TX. January.

Johnson, J., G. Wilson, A. Wentland, W. -C. Hsieh, and G. Yarwood. 2016b. "Daily Near Real-Time Ozone Modeling for Texas." Prepared for Texas Commission on Environmental Quality (TCEQ), TX. December.

Johnson, J., G. Wilson, M. Jimenez, T. Shah, R. Beardsley and G. Yarwood. 2017. "Fire Impact Modeling with CAMx." Prepared for Texas Commission on Environmental Quality (TCEQ), TX. July.

Kota, S. H., G. Schade, M. Estes, D. Boyer, Q. Ying. 2015. Evaluation of MEGAN predicted biogenic isoprene emissions at urban locations in Southeast Texas, Atmos. Environ., 110, 54-64. doi:10.1016/j.atmosenv.2015.03.027.

McDonald-Buller, E., Y. Kimura, C. Wiedinmyer, C. Emery, Z. Liu and G. Yarwood. 2015. Targeted Improvements in the Fire INventory from NCAR (FINN) Model for Texas Air Quality Planning. Prepared for David Sullivan, Texas Air Quality Research Program and The University of Texas at Austin. August.

McNally, D. E., 2009. "12km MM5 Performance Goals." Presentation to the Ad-Hoc Meteorology Group. 25-June. (http://www.epa.gov/scram001/adhoc/mcnally2009.pdf).

Ramboll, 2017. The User's Guide to the Comprehensive Air Quality Model with Extensions Version 6.40. Available from Ramboll, 773 San Marin Drive, Novato, CA. 94998 and at http://www.camx.com.

Shah, T., L. Parker, J. Grant and Greg Yarwood. 2018. "Modeling Inventories for Mexico and Caribbean Countries to Support Quantitative Analysis of International Transport Impacts on Ozone Design Values and Regional Haze." Prepared for Texas Commission on Environmental Quality (TCEQ), TX. June.

Skamarock, W.C., J.B. Klemp, J. Dudhia, D.O. Gill, D.M. Barker, M.G. Duda, X-Y Huang, W. Wang, J.G. Powers. 2008. "A Description of the Advanced Research WRF Version 3." NCAR Technical Note, NCAR/TN-45+STR (June 2008). http://www.mmm.ucar.edu/wrf/users/.

Stoeckenius, T.E., Emery, C.A., Shah, T.P., Johnson, J.R., Parker, L.K., Pollack, A.K., 2009. Air Quality Modeling Study for the Four Corners Region. Prepared for the New Mexico Environment Department, Air Quality Bureau, Santa Fe, NM. ENVIRON International Corporation, Novato, CA.

Wiedinmyer, C., Akagi, S. K., Yokelson, R. J., Emmons, L. K., Al-Saadi, J. A., Orlando, J. J., and Soja, A. J.: The Fire INventory from NCAR (FINN): a high resolution global model to estimate the emissions from open burning, Geosci. Model Dev., 4, 625-641, doi:10.5194/gmd-4-625-2011, 2011.

Wesely, M. L.: Parameterization of surface resistances to gaseous dry deposition in regional-scale numerical models, Atmos. Environ., 23, 1293–1304, 1989.

Wu, Z., Schwede, D.B., Vet, R., Walker, J.T., Shaw, M., Staebler, R. and Zhang, L., 2018. Evaluation and intercomparison of five North American dry deposition algorithms at a mixed forest site. Journal of Advances in Modeling Earth Systems. doi: 10.1029/2017MS001231.

Yu, H., A. Guenther, C. Warneke, J. de Gouw, S. Kemball-Cook, J. Jung, J. Johnson, Z. Liu, and G. Yarwood, 2015. "Improved Land Cover and Emission Factor Inputs for Estimating Biogenic Isoprene and Monoterpene Emissions for Texas Air Quality Simulations". Prepared for Texas Air Quality Research Program. (AQRP Project 14-016, September 2015).